

Thermodynamics of Fluid Polyamorphism

Mikhail A. Anisimov^{1,2*}, Michal Duška^{1,3}, Frédéric Caupin⁴, Lauren E. Amrhein¹,
Amanda Rosenbaum¹, and Richard J. Sadus⁵

¹*Department of Chemical & Biomolecular Engineering and Institute for Physical Science & Technology,
University of Maryland, College Park, U.S.A.*

²*Oil and Gas Research Institute of the Russian Academy of Sciences, Moscow, 117333, Russia*

³*Institute of Thermomechanics of the Czech Academy of Sciences, 182 00 Prague 8, Czech Republic*

⁴*Univ Lyon, Université Claude Bernard Lyon 1, CNRS, Institut Lumière Matière, F-69622, Lyon, France*

⁵*Centre for Molecular Simulation, Swinburne University of Technology, Hawthorn, Victoria 3122,
Australia*

“Fluid polyamorphism” is the existence of two alternative amorphous structures in a single-component fluid. It is either found or predicted, usually at extreme conditions, for a broad group of very different materials, including helium, sulfur, phosphorous, carbon, silicon, cerium, tin tetraiodide, tellurium, and hydrogen. This phenomenon is also hypothesized for metastable and deeply supercooled water, presumably located a few degrees below the experimental limit of homogeneous ice formation. We present a generic phenomenological approach to describe polyamorphism in a single-component fluid, which is completely independent of the molecular origin of the phenomenon. We show that fluid polyamorphism occurs either in the presence or the absence of fluid phase separation. In the latter case, it is associated with a continuous transition, such as in liquid helium or liquid sulfur. To specify the phenomenology, we consider a fluid with thermodynamic equilibrium between two distinct interconvertible states or molecular structures. A fundamental signature of fluid polyamorphism is the identification of the equilibrium fraction of molecules involved in each of these alternative structures. However, the existence of the alternative structures may result in polyamorphic fluid phase separation only if the mixing of these structures is not ideal. The two-state thermodynamics unifies all the debated scenarios of fluid polyamorphism with or without phase separation and qualitatively describes the thermodynamic anomalies typically observed in polyamorphic materials.

Subject Areas: Thermodynamics, Statistical Physics, Phase Transitions, Fluids

*To whom correspondence should be addressed. Email: anisimov@umd.edu.

I. INTRODUCTION

“Fluid polyamorphism” is the existence of two alternative amorphous structures in a single-component fluid [1-4]. The possibility of a liquid-liquid transition in a pure substance in addition to ordinary vapor-liquid separation is commonly considered as the signature of fluid polyamorphism [3-5]. However, different amorphous phases can also exist in single-component fluids without liquid-liquid separation [6-10] resulting in a continuous (second-order) phase transition. Fluid polyamorphism is found or predicted in a broad group of very different materials, such as helium [6, 7], sulfur [8-10], phosphorous [11], carbon [12], cerium [13], silicon [14-17], silicon dioxide [18-20], tellurium [21-23], tin tetraiodide [24, 25], and hydrogen [26-28]. Significantly, it has been also hypothesized in metastable and deeply supercooled water [29-34]. Two alternative forms of molecular arrangements are assumed to exist in supercooled liquid water: a low-density structure and a high-density structure. The existence of these two alternative structures could, under certain conditions, result in a metastable liquid-liquid separation in pure water. The hypothesized liquid-liquid metastable coexistence is not directly accessible in bulk-water experiments because it is presumably located a few degrees below the kinetic limit of homogeneous ice formation [34, 35]. Such coexistence has been reported for some atomistic water models (see review [34]), most notably in molecular simulations of the ST2 model [36]. A phase diagram similar to that predicted for water is found for a supercooled silicon model for which the liquid-liquid transition line continues to negative pressures in the doubly metastable region [20].

At high temperature and pressures of hundreds of GPa, highly compressed fluid hydrogen occurs in two forms: atomistic, metallic hydrogen and molecular, nonmetallic hydrogen [26-28]. The chemical reaction $NA \rightleftharpoons B$ is accompanied by a first-order fluid-fluid transition. It is expected that the fluid-fluid transition line is terminated at a critical point, above which there is a gradual transformation between the two forms of highly compressed hydrogen. A mixture of two interconvertible hydrogen species can be considered thermodynamically as a single-component fluid because the number of degrees of freedom is constrained by the condition of chemical-reaction equilibrium.

Liquid helium and sulfur represent two well-studied examples of fluid polyamorphism without phase separation. The “lambda transition” at ~ 2 K in ^4He , between the normal fluid and superfluid phases is a second-order transition caused by quantum Bose condensation [6]. Returning

to phenomena at higher temperatures, liquid sulfur is sharply polymerized at ~ 433 K [8-10]. When the degree of polymerization N is very large, the equilibrium reaction of polymerization $NA \rightleftharpoons B$ can be considered as a second-order phase transition between the monomer phase and the solution of polymer in monomers. Phosphorous is another example of polyamorphism driven by polymerization, though is not as well-studied [11].

A fundamentally important question is: what, if anything, is common to all the chemically very different systems exhibiting polyamorphism? In this work, we present a generic phenomenological approach, based on the Landau theory of phase transitions [37], to describe fluid polyamorphism in a single-component substance. This approach is completely independent of the underlying molecular nature of the phenomenon. To specify this approach and calculate phase behavior and thermodynamic properties, we consider a fluid with thermodynamic equilibrium between two competing interconvertible molecular “states” or structures.

The idea that water is a “mixture” of two different structures dates back to the 19th century [38,39]. Rapoport used two competing liquid structures to explain high pressure melting curve maxima at high pressures in some liquid metals [40]. More recently, the concept of two states (or three states if vapor is included) has become popular to explain liquid polyamorphism in cerium [13], tellurium [21-23], tin tetraiodide [24, 25], and water [41-47]. In a series of works by Tanaka et al., the idea of two competing liquid states was specified in terms of the alternative locally favored structures and two order parameters associated with these structures [48-51]. Most of the previously reported versions of two-state thermodynamics considered only liquid-liquid separation and ignored vapor-liquid transition or introduced it empirically as a background part of the Gibbs energy.

The phenomenology developed in our work encompasses the earlier approaches and opens the way to construct global equations of state for various polyamorphic materials of very different nature. We propose a mean-field equation of state that generically describes both vapor-liquid and liquid-liquid transitions in the same single-component fluid. Importantly, the equation of state is also valid for negative pressures. Negative pressures are observed and studied experimentally, particularly in water [52-54], and as such they are not simply a theoretical curiosity. A second-order phase transition, causing fluid polyamorphism without fluid-fluid separation, is also described by the generic phenomenology. Furthermore, we discuss two alternative mechanisms for a liquid-liquid transition in a single-component fluid. The “discrete” mechanism is driven by

the existence of two distinct mixable/unmixable molecular or supramolecular structures. In contrast, the “continuous” mechanism, associated with isotropic two-scale nonideality in the Gibbs energy does not contain the entropy of mixing of two alternative entities. Thermodynamically, these cases may produce similar phase diagrams and similar property anomalies. Discrimination of these mechanisms can be made by further examining structural properties and dynamics of structural relaxation.

II. RESULTS

a. Generic formulation of polyamorphism in a single-component fluid

A generic thermodynamic description of fluid polyamorphism can be formulated by using the Landau theory of phase transitions [37], in which the key concept is the order parameter, a variable that characterizes the emergence of a more ordered state. The Gibbs energy (per molecule) G of a single-component fluid is generally presented in the form

$$G(p, T, \phi) = G_o(p, T) + kTf(\phi) - h\phi, \quad (1)$$

where p , T and k are the pressure, temperature and Boltzmann’s constant, respectively. In Eq. (1), ϕ is the order parameter. The variable h is a thermodynamic field conjugate to the order parameter known as the “ordering field,” and $f(\phi)$ is a function whose specific form depends on the molecular nature of the order parameter. If the order parameter is a vector, the ordering field is also a vector. In this case the order parameter breaks the symmetry of the disordered state. We must note that Eq. (1) applies to phenomena and systems with both different physical nature of the order parameter and, correspondingly, ordering field. In some cases such as magnetization, the ordering field (i.e., the magnetic field) is an independent variable, whereas generally in polyamorphic fluids the ordering field may be a function of pressure and temperature. It is also possible that some polyamorphic transitions occur only in zero ordering field because the state with non-zero field does not physically exist, e.g., the lambda transition in He^4 [6]. We emphasize

that in our approach we include the ordinary vapor-liquid transition in the “background” part of the Gibbs energy $G_o(p, T)$ that is independent of ϕ .

The equilibrium value of the order parameter is found by minimizing the Gibbs energy via $(\partial G / \partial \phi)_{p, T} = 0$. This minimization results in the equilibrium condition $h(p, T) = (\partial f / \partial \phi)_{p, T}$ and thus makes the equilibrium value of the order parameter, $\phi = \phi_e$, to be a function of p and T . A particular form of $\phi = \phi_e$ depends on the nature of the order parameter. Generally, one can define $\phi_e(p, T)$ to vary between zero (alternative amorphous structure is absent) and unity (fully developed alternative amorphous structure).

b. Fluid polyamorphism induced by thermodynamic equilibrium between interconvertible molecular states

To enable the general formulation of fluid polyamorphism for the calculation of thermodynamic properties, we need to specify the nature of the order parameter and, consequently, the explicit form of the function $f(\phi)$. One attractive scenario is thermodynamic equilibrium between two alternative interconvertible molecular states or supramolecular structures. This scenario is phenomenologically equivalent to “chemical-reaction” equilibrium between two alternative “species”, A and B. We do not need to specify the atomistic structure of these states. They can be two different structures of the same molecule (isomers), dissociates and associates, or two alternative supramolecular structures, such as different forms of a hydrogen-bond network. Hence, the conversion of one molecular or supramolecular state to another one may not necessarily require breaking of chemical bonds.

Let x be the fraction of the state B in the “chemical reaction” $A \rightleftharpoons B$. This variable is also known as the “reaction coordinate” or “degree of reaction” [55]. In chemical reactions the number of atoms is conserved while number of molecules may or may not be conserved. The conservation of the number of atoms is controlled by stoichiometric coefficients. For simplicity, we first consider equal stoichiometric coefficients for A and B, meaning that the number of molecules in the reaction is conserved. Generally, the reaction $A \rightleftharpoons B$ may involve different

stoichiometric coefficients ν_A and ν_B (such as $2H \rightleftharpoons H_2$ or, generally, $\nu_A A \rightleftharpoons \nu_B B$). Specific stoichiometry may modify the relation between the reaction coordinate and the molecular fraction of each state and separate the condition of reaction equilibrium and the condition of phase equilibrium.

We specify the Gibbs energy (per molecule) given by Eq. (1) in the form

$$G = G_A + xG_{BA} + G_{\text{mix}}, \quad (2)$$

where $G_{BA} = G_B - G_A$, the difference between the Gibbs energies of the molecular entities B and A, is equivalent to $-h$, while G_{mix} , the Gibbs energy of mixing, is equal to $kTf(\phi)$. Furthermore, G_A can be identified with G_0 , and x , the molecular fraction of state B, with the order parameter ϕ .

Adopting in this section a symmetric form of the Gibbs energy of mixing, $G_{\text{mix}} = H_{\text{mix}} - TS_{\text{mix}}$ (where H_{mix} is the enthalpy of mixing and S_{mix} is the entropy of mixing), such that $H_{\text{mix}} - TS_{\text{mix}} = \omega x(1-x) + kTx \ln(x) + kT(1-x) \ln(1-x)$, we write [55]

$$G(p, T, x) = G_A(p, T) + xG_{BA}(p, T) + kTx \ln(x) + kT(1-x) \ln(1-x) + \omega x(1-x), \quad (3)$$

where ω is the parameter of nonideality of mixing. In general, ω is a function of T and p . The ideal-solution mixing in the Gibbs energy of mixing is represented by the “ideal-gas” entropy $S_{\text{mix}}^{\text{ideal}} = -k[x \ln(x) + (1-x) \ln(1-x)]$. If ω does not depend on T , being a system-dependent constant, or depends only on p , the nonideality $G_{\text{mix}} - TS_{\text{mix}}^{\text{ideal}} = \omega x(1-x)$ is entirely enthalpy driven (“regular mixing”). If ω is simply proportional to T , while being arbitrarily dependent on p , the nonideality is entirely entropy driven (“athermal mixing”). In most real mixtures, nonideality is driven by both, enthalpy and entropy. For simplicity, in this section, we consider ω to be a constant.

The molecular fraction of state B (i.e., x), is also the reaction coordinate. The equilibrium value of the reaction coordinate in this particular formulation is equivalent to the equilibrium value of the order parameter ϕ . The chemical reaction equilibrium between A and B makes the mixture of A and B equivalent thermodynamically to a single-component fluid. Indeed, the equilibrium

value of the reaction coordinate $x = x_e(T, p)$, the fraction of molecules involved in state B, is obtained from the condition of chemical reaction equilibrium [37, 55]

$$\left(\frac{\partial(G/kT)}{\partial x} \right)_{p,T} = 0, \quad (4)$$

yielding the explicit relation between the order parameter and the ordering field:

$$h = kT \ln K(p, T) = -G_{BA}(p, T) = kT \ln \frac{x}{1-x} + \omega(1-2x), \quad (5)$$

where $K(T, P)$ is the reaction equilibrium constant. In a binary mixture without chemical equilibrium, the difference between the Gibbs energies G_{BA} depends on an arbitrary constant because G_A and G_B are independent. The chemical-equilibrium condition (4) eliminates this uncertainty, thus making G_{BA} well defined.

An important practical question arises: under which experimental conditions will the system described by Eq. (3) behave either as a binary fluid mixture or as a single-component fluid? The answer depends on the separation of time scales: a system with two inter-convertible fluid structures can be thermodynamically treated as a single-component fluid if the time of observation is longer than the characteristic time of reaction (fast conversion). In the opposite limit (slow conversion) the system behaves thermodynamically as a two-component mixture. In this case, the constraint imposed by Eq. (4) does not apply and the concentration of the species becomes an independent variable. Therefore, applying the “chemical-reaction” approach for the description of fluid polyamorphism assumes that the conversion is fast enough to satisfy the equilibrium condition (4) within the experimental time scale.

We emphasize that our use of the term “chemical-reaction equilibrium” does not necessarily imply that polyamorphism and liquid-liquid separation in a pure fluid involves a chemical reaction in the conventional definition, i.e., breaking of chemical bonds. Within the framework of Landau theory of polyamorphism, this terminology is phenomenologically equivalent to the condition of thermodynamic equilibrium with the Gibbs energy containing the ideal entropy of mixing of two distinct alternative states and the nonideal (“excess”) Gibbs energy of mixing.

c. Polyamorphic fluid-fluid phase separation

We note that for the symmetric Gibbs energy of mixing given by Eq. (3) the condition $\ln K(p, T) = 0$ and the condition of phase equilibrium (zero ordering field) coincide. Along the line $\ln K(p, T) = 0$, if $\omega / k_B T \leq 2$, there is only one solution of Eq. (5), that is $x = 1/2$. However, if $\omega / k_B T > 2$, this equation has two stable solutions, $x > 1/2$ and $1 - x < 1/2$. This corresponds to the coexistence of two fluid phases enriched with either A or B. This means that the line $\ln K(T, P) = 0$ is the fluid-fluid phase transition line. The temperature

$$T_c^* = \frac{\omega}{2k} \quad (6)$$

is the critical temperature for the polyamorphic fluid-fluid transition. The critical pressure p_c^* , is found from the condition $\ln K(T = T_c^*, p = p_c^*) = 0$. The temperature of the fluid-fluid coexistence as a function of the fraction of state B is found as

$$\hat{T}_{\text{cxc}} = \frac{2(2x-1)}{\ln x(1-x)}, \quad (7)$$

where $\hat{T}_{\text{cxc}} = T_{\text{cxc}} / T_c^*$. At the critical point $x = x_c = 1/2$. Above the critical temperature, the line $\ln K(p, T) = 0$ (a continuation of the line of phase transitions, along which $x = 1/2$) is known as the Widom line.

Equation (7) is equivalent to the temperature-dependence of the spontaneous (in zero field) order parameter obtained in the mean-field approximation for the Ising/lattice gas model. Indeed, introducing $M = 2x - 1$ and using $\text{arctanh}(M) = \frac{1}{2} \ln \frac{1+M}{1-M}$, we obtain the well-known Ising-model mean-field result [56]:

$$M = \tanh \frac{M}{\hat{T}_{\text{cxc}}}. \quad (8)$$

Expansion of Eq. (8) in powers of M in the vicinity of the critical point yields the asymptotic power law in the meanfield approximation: $M = 2x - 1 = \pm \left[3(T - T_c^*) / T_c^* \right]^{1/2}$.

d. Calculation of thermodynamic properties

From Eq. (3), we can obtain

$$\frac{\partial x}{\partial p} G_{\text{BA}} + kT \frac{\partial}{\partial p} \left[x \ln x + (1-x) \ln(1-x) + \omega x(1-x) \right] = 0, \quad (9)$$

and

$$\frac{\partial x}{\partial T} G_{\text{BA}} + k \frac{\partial}{\partial T} \left[x \ln x + (1-x) \ln(1-x) + \omega x(1-x) \right] = 0. \quad (10)$$

The density and entropy are calculated from

$$\rho(p, T) = \frac{1}{V(p, T)} = \left(\frac{\partial G}{\partial p} \right)_T^{-1} = \frac{1}{V_A(p, T) - kT (\partial \ln K / \partial p) x(p, T)}, \quad (11)$$

and

$$S(p, T) = - \left(\frac{\partial G}{\partial T} \right)_p = S_A(p, T) + k (\partial \ln K / \partial T) x(p, T), \quad (12)$$

where $V_A = V_A(p, T)$ and $S_A(p, T)$ are the volume and entropy (per molecule) of state A.

Analogously, from the Gibbs energy, if state A and $\ln K(T, P)$ are specified we can obtain all other thermodynamic properties, such as the isothermal compressibility and heat capacity, as well as the global phase diagram that includes both vapor-liquid and liquid-liquid transitions.

e. Specifying state A and equilibrium constant

We have used two alternative choices of $G_A(p, T)$. One option is to adopt the chemical potential of the lattice-gas model $G_A = \mu_{\text{lg}}$. The other option is to use the chemical potential of

the van der Waals fluid $G_A = \mu_{\text{vdw}}$. Both these models famously describe the transition between liquid and gaseous states and vapor-liquid coexistence. However, there is an important conceptual difference between these two models: lattice gas is a discrete model consisting of two distinct states (empty cells and occupied cells) with the entropy mathematically equivalent to the entropy of mixing in a binary fluid. The van der Waals fluid is a continuous model without distinct alternative states. In the Supplemental Material (Section 1), we provide details of thermodynamic equations for the lattice-gas and van der Waals models, as well as for the fine lattice discretization model (Section 2) that uniformly describes crossover between the two alternative models [57]. The effect of the differences in these two alternative formulations of state A on the global phase diagram and properties of a polyamorphic fluid are not significant. Major effects are caused by a particular dependence of the equilibrium constant on p and T and by the distance from the liquid-liquid critical point to the absolute stability limit of the liquid state with respect to vapor (the liquid branch of the vapor-liquid spinodal).

The formulation on an explicit equation of state requires the specification of the equilibrium constant $K(T, P)$. A general form of the Gibbs energy change of reaction can be represented by the polynomial

$$G_{\text{BA}}(p, T) = -kT \ln K(T, P) = k(\lambda + \alpha p + \beta T + \chi p T + \delta p^2 + \varepsilon T^2 + \dots). \quad (13)$$

Correspondingly, for the equilibrium constant:

$$\ln K(p, T) = \frac{G_{\text{BA}}}{kT} = \frac{\lambda}{T} + \alpha \frac{p}{T} + \beta + \chi p + \delta T + \varepsilon \frac{p^2}{T} + \dots, \quad (14)$$

where the coefficients of the polynomial represent the changes (in first approximation) of energy (λ), volume (α), entropy (β), isobaric expansivity (χ), heat capacity (δ), and isothermal compressibility (ε) in the reaction $A \rightleftharpoons B$. In the linear approximation,

$$G_{\text{BA}}(p, T) = k(\lambda + \alpha p + \beta T). \quad (15)$$

In this approximation the conversion between two states is only affected by changes in energy, volume, and entropy. The phase transition line and the Widom line are defined as $\lambda + \alpha p + \beta T = 0$ with a constant slope $dp/dT = S_{\text{BA}}/V_{\text{BA}} = -\beta/\alpha$. In the Supplemental Material (Section 3) we report the results for an alternative form of the equilibrium constant. These results support our conclusion on the generic character of the developed approach.

f. Global phase diagrams and lines of extrema of thermodynamic properties

In this section we present results obtained by using $G_A(p, T)$ for the chemical potential of the lattice-gas model. Essentially similar results, presented in the Supplemental Material, are obtained when adopting $G_A(p, T)$ for the chemical potential of the van der Waals model.

A typical phase diagram, calculated from Eq. (3) with $G_{BA}(p, T)$ using the linear approximation given by Eq. (15), for the polyamorphic lattice-gas model is presented in figures 1a and 1b. Dimensionless values of temperature (\hat{T}) and pressure (\hat{p}) are relative to the critical parameters of the vapor-liquid critical point (CP1). The parameters of the model for this particular case are, $\lambda / kT_{cl} = 0.5$, $\alpha / \rho_{cl} kT_{cl} = -0.05$, $\beta / k = -1.5$, and $\omega / kT_{cl} = 0.6$. Figures 1a and 1b show the vapor-liquid and liquid-liquid coexistence (with the liquid-liquid critical point, CP2, as a simple example located at a positive pressure for the selected parameters), the absolute stability limit of the liquid state with respect to vapor, and the Widom line. The right branch of the vapor-liquid spinodal, which is the absolute stability limit of liquid with respect to vapor (obtained as the locus of maxima of the isobars), demonstrates re-entrant behavior at the densities close to the liquid-liquid critical density.

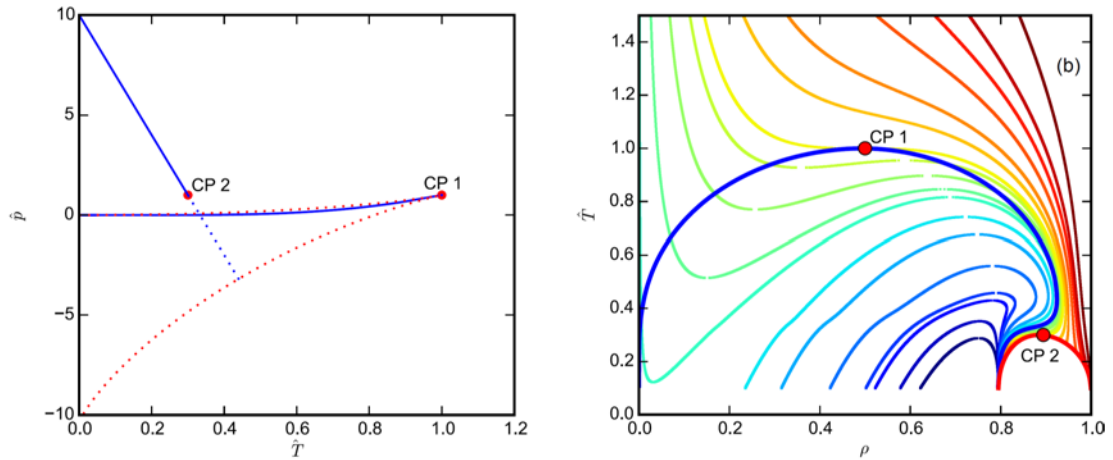


Figure 1. Phase diagram for a polyamorphic lattice gas; $\hat{T} = T / T_{cl}$ and $\hat{p} = p / p_{cl}$. (a) Pressure/temperature diagram. Blue line and blue curve are vapor-liquid and liquid-liquid transitions; CP1 and CP2 are the vapor-liquid and liquid-liquid critical points assigned (as an example) to be at the same isobar. Red dotted curves are the liquid and vapor branches of liquid-vapor spinodal). Blue dotted line is the Widom line. (b) Temperature/density diagram. Thick blue curve is the vapor-liquid coexistence, thick red curve is the liquid-liquid coexistence. Multicolor curves are selected isobars.

Figure 2 demonstrates an example of the behavior of the isothermal compressibility along three selected isobars: above the liquid-liquid critical pressure that for this particular case is selected equal for both CP1 and CP2 (green), at the critical pressure (red), and below the critical pressure (blue). One may notice the divergence of the isothermal compressibility at the critical points and at the vapor-liquid spinodal.

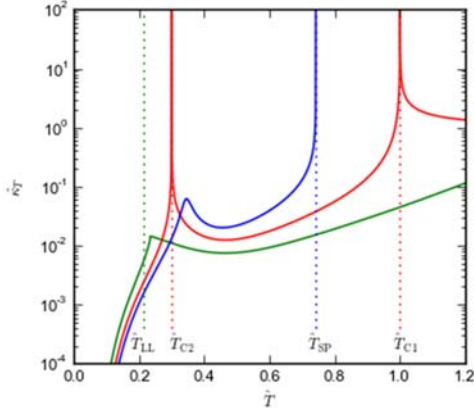


Figure 2. The dimensionless isothermal compressibility $\hat{\kappa}_T = \rho^{-1}(\partial \rho / \partial \hat{p})$ along three selected isobars: above the liquid-liquid critical pressure, assigned equal to the vapor-liquid critical pressure, (green), at the critical pressure (red), and below the critical pressure (blue). $\hat{T}_{c1} = 1$ and $\hat{T}_{c2} = T_{c2} / T_{c1}$ are the vapor-liquid and liquid-liquid critical temperatures, $\hat{T}_{LL} = T_{LL} / T_{c1}$ is the temperature of the liquid-liquid transition at the selected isobar.

The location of the liquid-liquid critical point depends on the interplay of two essential parameters, λ (the energy change of reaction at zero pressure) and $\omega = 2kT_{c2}$ (the nonideality of mixing of the alternative states). As shown in Figure 3, by tuning $T_{c2} = \omega / 2k$ from zero to a certain positive value (depending on λ) the model evolves from a “singularity-free” scenario ($T_{c2} = 0$) to a “critical-point-free” scenario (the liquid-liquid critical point is located beyond the absolute stability limit of liquid state with respect to vapor).

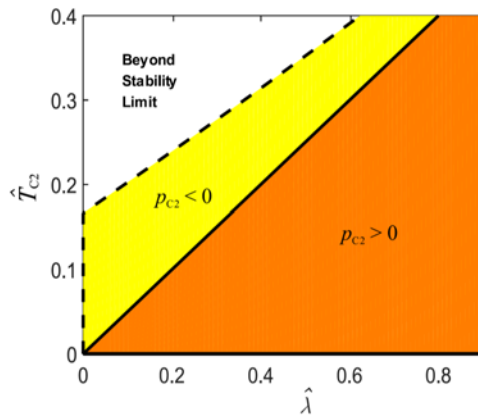


Figure 3. Parameterized phase diagram for polyamorphic lattice gas in terms of nonideality of mixing of the alternative states A and B, $\hat{T}_{c2} = \omega / 2kT_{c1}$, and the energy difference of A and B, $\hat{\lambda} = \lambda / kT_{c1}$. The volume difference of states A and B is taken constant. The singularity-free scenario corresponds to $\hat{T}_{c2} = 0$. The critical point-free scenario is favored by stronger nonideality and smaller energy difference.

Stokely et al. [58] studied the effects of hydrogen bond cooperativity on the behavior of supercooled water. The authors introduced two major parameters: the strength of the directional component of the hydrogen bond and the degree of hydrogen bond cooperativity. If the degree of hydrogen bond cooperativity is zero, the neighboring bonds are formed independently. We note that if the strength of the directional component of the hydrogen bond is identified with the energy change of reaction (λ) and the degree of the cooperative component of the hydrogen bond is identified with the nonideality parameter $\omega \propto T_{c2}$ then the phase diagram presented in Figure 3 is virtually the same as that obtained by Stokely et al.

Tuning the distance of the liquid-liquid critical point from the absolute stability limit of the liquid state with respect to vapor results in dramatic change in thermodynamic behavior of the system and, especially, in the pattern of extrema in thermodynamic properties [59, 60]. In particular, the locus of density maximum/minimum is one of the most characteristic features of polyamorphic liquids. The salient points of this locus are interrelated, through thermodynamic relations, with the extrema loci of thermodynamic response functions, such as the isothermal compressibility along isobars or the isobaric heat capacity along isotherms [60, 61]. Furthermore, since the extrema loci are experimentally observed for a broad range of temperatures and pressures, including thermodynamically stable regions, their shape is important information for modelling liquid polyamorphism, especially if the liquid-liquid transition is experimentally inaccessible [62].

The evolution of the extrema loci upon tuning the location of the liquid-liquid critical point is demonstrated in Figure 4 from (a) (“singularity-free scenario”) to (d) (“critical-point-free scenario”). The pattern of extrema loci in Figure 4a demonstrates a singularity-free scenario [59] which is relevant to those tetrahedral system that do not exhibit a metastable liquid-liquid separation, such as the mW model of water [63]. The pattern presented in Figure 4b (a “regular” scenario, the liquid-liquid critical point is located at a positive pressure) is observed in the popular ST2 [64] and TIP4P/2005 [65] atomistic water models. The additional (shallow) extrema of the heat capacity, observed in this case, is unrelated to the liquid-liquid transition and is specific to the model adopted for state A. The extrema are also unrelated to so-called “weak” extrema of the heat capacity and isothermal compressibility reported by Mazza et al. [66], which emanate from the liquid-liquid critical point and which are specific for their “many-body model” of water. The case presented in Figure 4c is a degenerate one as the critical point coincides with the vapor-liquid spinodal. Finally, Figure 4d presents the case in which the transition line remains of first-order

until the liquid becomes unstable with respect to vapor (“critical-point-free scenario”). One can notice that the vapor-liquid spinodal remains continuous even when it intercepts the liquid-liquid transition line. This is because of the linear form of $G_{BA}(T, p)$, given by Eq. (15), that was used for the calculations. This form implies that the compressibility of states A and B is the same.

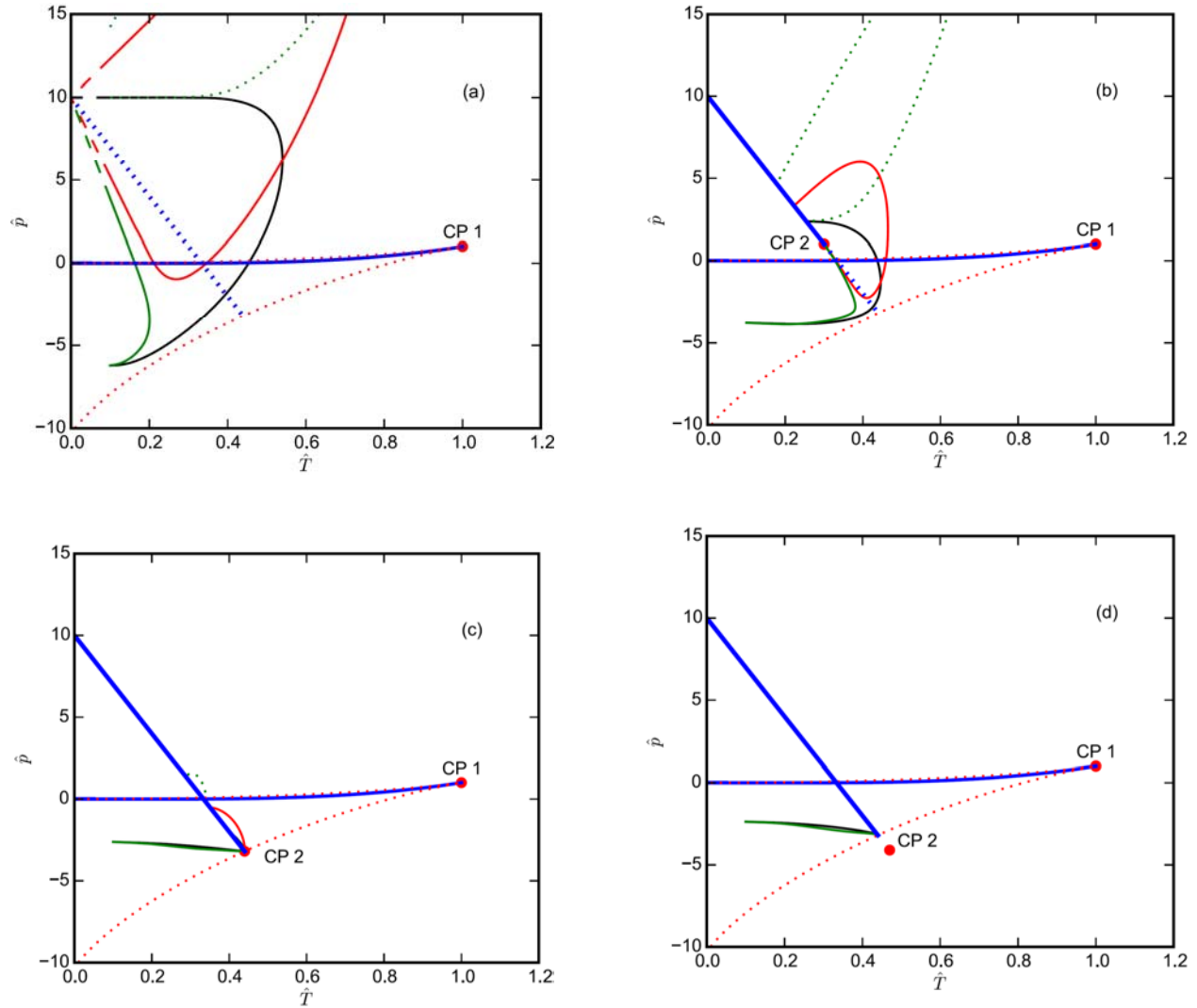


Figure 4. Evolution of the pattern of the extrema loci upon tuning the location of the liquid-liquid critical point. Black is the density maximum or minimum; red is the isothermal compressibility maximum or minimum along isobars, green is the isobaric heat capacity maximum or minimum along isotherms; dotted green shows additional (shallow) extrema of the heat capacity unrelated to the liquid-liquid transition; dotted red are two branched of the liquid-vapor spinodal; blue dashed is the Widom line; red dots are the vapor-liquid (CP1) is the liquid-liquid critical point (CP2). (a) a “singularity-free” scenario – the critical point is at zero temperature, thus it is not labeled as CP2; extrapolations of the extrema loci to zero temperature are shown as dashed lines; (b) a “regular” scenario – the critical point CP2 is at a positive pressure; (c) the critical point coincides with the absolute stability limit of the liquid state; (d) a “critical point-free” scenario – the “virtual” critical point CP2 is located in the unstable region.

The most dramatic result of the evolution of the extrema loci is the shrinking and eventual disappearance of the maximum density locus upon the transition from the singularity-free scenario to the critical-point-free scenario. This effect appears to be generic because it is qualitatively observed for both choices of state A, the lattice gas and van der Waals models, with various sets of the model parameters (see Supplemental Material, figures S9 and S10) and has been recently observed in the doubly metastable silica [67]. Other, specific to different polyamorphic materials, equations for State A are worth to consider in further studies.

Another remarkable peculiarity of liquid polyamorphism, which has not been reported previously in the literature, is a singularity (“bird’s beak”) in the liquid-liquid coexistence curve when the critical point coincides with the liquid-vapor spinodal (Figure 4b). This singularity is associated with the common tangent of the liquid-liquid coexistence and vapor-liquid spinodal as it is demonstrated in Figure 5 (a) and (b). This effect is generic as it is also observed for the van der Waals choice for state A (see Supplemental Material, figure S11). A similar shape for fluid-fluid coexistence is observed in dilute binary solutions near the vapor-liquid critical point of the pure solvent [68].

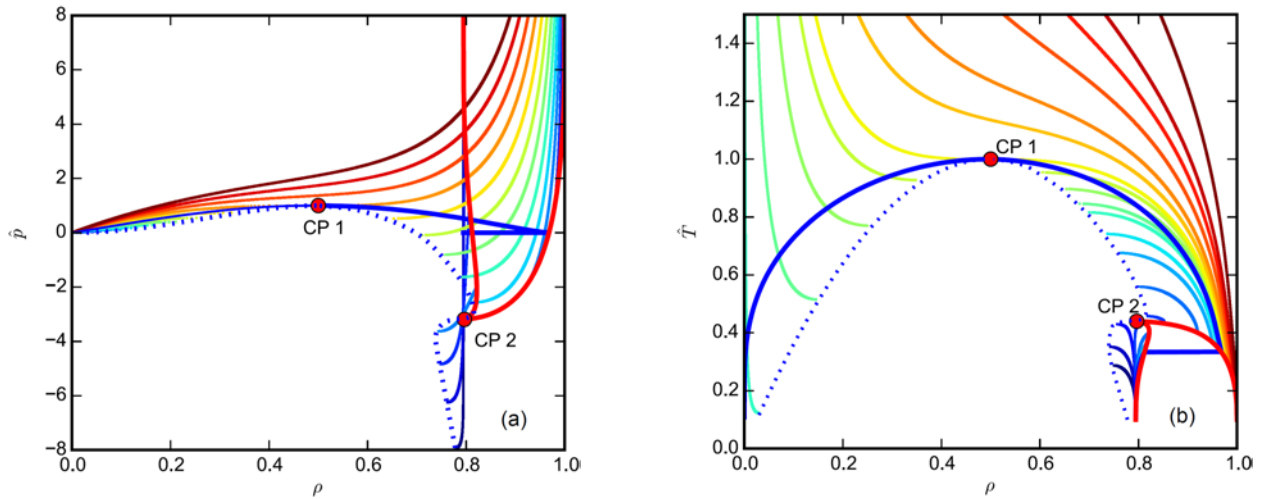


Figure 5. A singularity (“bird’s beak”) in the liquid-liquid coexistence curve if the critical point coincides with the liquid-vapor spinodal. (a) $p - \rho$ diagram, (b) $T - \rho$ diagram. Thick blue curve is the vapor-liquid coexistence; thick red is the liquid-liquid coexistence; CP1 and CP2 are the vapor-liquid and liquid-liquid critical points, respectively; dotted blue is the liquid-vapor spinodal; multicolor curves are selected isotherms (a) and selected isobars (b).

g. Fluid polyamorphism without phase separation: superfluid transition in liquid helium

Second-order phase transitions (“lambda transitions”) of superfluidity in the ^4He and ^3He helium isotopes, are arguably the most famous examples of liquid polyamorphism without phase separation [6, 7]. The formation of the superfluid is associated with the formation of a Bose-Einstein condensate. In ^4He , the lambda transition between the normal fluid and superfluid phases occurs at ~ 2 K [6], while ^3He forms a superfluid phase (A or B, depending on pressure) at a temperature below 0.0025 K [7].

In the mean-field approximation, polyamorphism in helium is described near the transition temperature $T_\lambda(p)$ by Eq. (1) with $h(p, T) = |\mathbf{h}| = 0$, $\phi(p, T) = |\boldsymbol{\psi}|$ (a two-component vector order parameter, the wave function in the theory of Bose-Einstein condensation [6,7], containing real and imaginary parts) and $f(T, p)$ given by a Landau expansion [37]:

$$f(T, p) = \frac{1}{2} \frac{T - T_\lambda(p)}{T_\lambda(p)} |\boldsymbol{\psi}|^2 + \frac{1}{4} u |\boldsymbol{\psi}|^4, \quad (16)$$

where u is a coupling constant. The superfluid phase below $T_\lambda(p)$ can be viewed phenomenologically as a two-state “mixture” with the fraction of the superfluid component controlled by thermodynamic equilibrium. The order parameter in the mean-field approximation changes with temperature as $|\boldsymbol{\psi}| = \pm \left[(1/u)(T_\lambda - T)/T_\lambda \right]^{1/2}$. In contrast, the experimentally observable physical property, the fraction of the superfluid component, is a scalar, changing along isobars as $\rho_{\text{sf}} \propto |\boldsymbol{\psi}|^2 \propto T_\lambda(p) - T$. The transition is continuous, occurring in pure helium without phase separation. However, liquid-liquid phase separation is observed in a mixture of ^4He and ^3He , where the lambda transition at the tricritical-point concentration of ^3He becomes a first-order transition [69]. The physical origin of tricriticality in the ^4He - ^3He mixture is the coupling between the vector order parameter $\boldsymbol{\psi}$ and concentration (a scalar) of ^3He [69,70]. One may note that the mean-field shape of the tricritical liquid-liquid coexistence, in contrast to the ordinary parabolic fluid-fluid coexistence, is angle-like as the difference of concentration of the mixture and its tricritical value $c - c_{\text{tct}} \propto \rho_{\text{sf}} \propto T_{\text{tct}} - T$.

h. Fluid polyamorphism caused by polymerization without or with phase separation

The transition to polymeric liquid sulfur at a temperature about ~ 433 K is another example of fluid polyamorphism without phase separation. The properties of sulfur near the polymerization transition are completely reversible as is the case for a continuous phase transition. Using a Heisenberg n -vector model in the limit $n \rightarrow 0$, Wheeler *et al.* [71, 72] explained the polymerization in sulfur as a second order phase transition in a weak external field. An earlier theory by Tobolsky and Eiseberg [8] describes the temperature dependence of the extent of polymerization in terms of a second order phase transition in the mean-field approximation. The situation in real sulfur may be more complicated because the polymerization occurs upon heating [8, 9] in the supramolecular structure of liquid sulfur containing octamers that are to be broken to undergo polymerization. Furthermore, according to Dudowicz *et al.* [73] polymerization in actin is equivalent to a thermodynamic phase transition only in the limit of zero concentration of the initiator.

Here we consider the simplest scenario, namely an equilibrium reaction of polymerization $NA \rightleftharpoons B$ in the liquid phase of monomers A. In the limit $N \rightarrow \infty$, this reaction is equivalent to a second-order phase transition in zero field between the phase containing only monomers (state A) and the phase containing a solution of the infinite polymer chain in the monomers (state B). The phenomenon is equivalent to a second-order transition because the volume fraction of polymer is continuous at the starting point of polymerization, while its derivative is discontinuous. For polymerization in an incompressible liquid system, the volume fraction of polymer is proportional to the fraction of polymerized monomers, x . If the solvent consists of nonpolymerized monomers, this transition is described thermodynamically by the Flory mean-field theory of polymer solutions [74, 75] constrained by the equilibrium reaction of polymerization. In the Flory theory, the Gibbs energy per monomer

$$G(p, T, x) = G_A + xG_{BA} + kT \frac{x}{N} \ln x + kT(1-x) \ln(1-x) + \omega x(1-x). \quad (17)$$

In the simplest approximation, the interaction parameter ω is assumed to be a constant, $\omega = \frac{k\Theta}{2}$, where Θ is a temperature of phase separation in the limit $N \rightarrow \infty$, $x \rightarrow 0$ (the theta temperature). At temperatures much higher than the theta temperature (when the interaction parameter is negligible), the infinite chain exhibits a self-avoiding walk in solution of monomers [76].

For a reversible reaction at the condition $\omega \ll kT$, the enthalpy of mixing can be neglected and the chemical-reaction equilibrium condition reads

$$G_{\text{BA}}(p, T) = \frac{kT}{N} - kT + \frac{kT}{N} \ln x - kT \ln(1-x). \quad (18)$$

Specifying the Gibbs energy change of reaction as $G_{\text{BA}}(p, T) = k(\lambda + \alpha p + \beta T)$, we obtain the temperature dependence of the polymer volume fraction along isobars, presented in Figure 6. At a finite degree of polymerization, there is no sharp transition between the monomer and polymer phases. This case corresponds to a “singularity-free” scenario in the two-state thermodynamics, even if the asymmetry in the equilibrium fraction is very strong at large N . However, in the limit $N \rightarrow \infty$ the polymer volume fraction is zero at all temperatures above the transition temperature, $T = T_\lambda(p)$, defined by the condition $\lambda + \alpha p + \beta T + kT = 0$. We note that in this, highly asymmetric, case the condition $\ln K = \lambda + \alpha p + \beta T = 0$ and the condition of phase equilibrium at the transition temperature, $\lambda + \alpha p + \beta T + kT = 0$ are not the same. One can also notice that near the transition temperature the polymer volume fraction changes linearly as a function of $T - T_\lambda(p)$, suggesting that, like in the cases of superfluidity, the order parameter for polymerization in the limit $N \rightarrow \infty$ is proportional to $x^{1/2}$.

Therefore, in this (asymmetric entropy-driven) case of fluid polyamorphism without phase separation, the nature of the order parameter is fundamentally different from the case of energy-driven polyamorphism (with phase separation when N and ω are finite) and for which the order parameter is a fraction of the polymerized monomers.

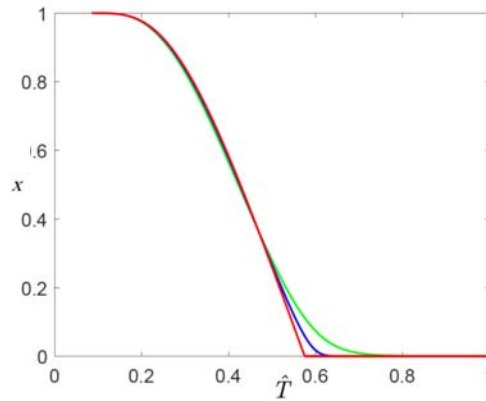


Figure 6. Fraction of polymerized monomers as a function of temperature for different degrees of polymerization. Green curve corresponds to $N = 10$, blue $N = 10$, and red $N \rightarrow \infty$. The polymerization in the limit $N \rightarrow \infty$ is equivalent to a continuous (second-order) phase transition in zero field.

Therefore, we note that the meaning of the order parameter for the system in which two interconvertible states are controlled by chemical-reaction equilibrium changes from the fraction of conversion for the symmetric case, given by Eq. (17) if $N=1$, to a specific vector-like order parameter associated with self-avoiding walk singularities of the infinitely long ($N \rightarrow \infty$) polymer chain [75-77].

Wheeler [78] also considered polymerization of sulfur in a molecular solvent. If the mutual attraction between the monomers fragments of the polymer chain is stronger than between the chain fragments and solvent molecules, at a certain temperature, analogous to the theta temperature, $\Theta = 2k\omega$, the transition to the polymer-rich phase could be accompanied by phase separation. A tricritical point is observed when the line of second-order phase transitions becomes the line of first-order transitions [69]. Therefore, the theta point of the infinite polymer chain in the solution of its equivalent to the tricritical point.

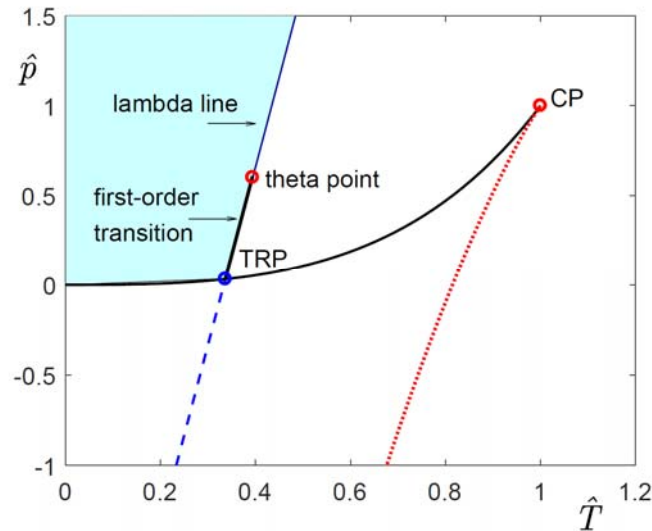


Figure 7. Generalized phase diagram of a fluid exhibiting equilibrium polymerization into an infinite chain. Blue area is the polymeric phase; Thick black line and curve are first-order phase transitions (coexistence between monomer and polymer phases and between vapor and liquid, respectively); CP is the vapor-liquid critical point; the theta point is equivalent to a tricritical point which separates the second-order and first order phase transitions; TRP is the triple point (monomers, polymer enriched phase, and vapor coexist). Dotted red curve represents the absolute stability limit of liquid with respect to vapor. Blue dashed line is continuation of the liquid-liquid transition line into the metastable region.

A similar phenomenon could, in principle, exist in a pure polymerizing molecular liquid if the attraction between the monomers fragments of the emerging polymer chain is stronger than between the chain fragments and the nonpolymerized monomers. Then the monomers and the

monomer solution enriched with the polymer will separate below the theta temperature (see figure S12 in the Supplemental material). The generalized phase diagram of a one-component fluid exhibiting polymerization into an infinite polymer chain with the possibility of phase separation below the theta point is presented in Figure 7. In practice, significant nonideality in interactions between the fragments of the polymer chain and its monomers seems rare, thus making the existence of the tricritical point in a polymerized one-component fluid an exotic phenomenon.

i. Liquid-liquid transition in a single component fluid without entropy of mixing discrete molecular states

In a single-component fluid, the existence of a liquid-liquid separation, in addition to the vapor-liquid transition, does not necessarily require the existence of distinct interconvertible molecules or molecular structures. Indeed, the Landau theory of phase transitions can phenomenologically describe this scenario without any reference to interconversion between alternative molecular states.

Let the Gibbs energy of a fluid be described by Eq. (1) with the ordering field $h(p, T)$. The ordinary vapor-liquid transition is described by $G_o(p, T)$. The origin of a possible liquid-liquid transition and the nature of the order parameter depends on a particular form of the function $f(\phi)$. If we adopt a continuous free-energy model for this function, e.g. in the form

$$f(\phi) = \phi \ln \frac{\phi}{1 - \tilde{b}\phi} - \frac{\tilde{a}\phi^2}{kT}. \quad (19)$$

The derivative of Eq. (19) yields the expression for the ordering field in the form of the chemical potential of a van der Waals fluid:

$$h = \frac{\partial f}{\partial \phi} = kT \left(\frac{1}{1 - \tilde{b}\phi} + \ln \frac{\phi}{1 - \tilde{b}\phi} \right) - 2\tilde{a}\phi, \quad (20)$$

where the interaction parameter \tilde{a} defines the second energy scale and \tilde{b} is the second distance scale. From Eq. (20), using a particular form of $h = h(T, p)$, e. g., $h = \lambda + \alpha P + \beta T$, one can obtain the equilibrium value of the order parameter $\phi_e = \phi(p, T)$.

We note that in this scenario the order parameter is not an equilibrium fraction of molecules involved in state B because there is no entropy of mixing of two distinct species in the function $f(\phi)$. Instead, the order parameter originates from the additional scales in the energy and distance in the intermolecular potential, being phenomenologically associated (in first approximation) with the excess entropy $S_{\text{ex}} = S - S_0 = -\beta\phi$ and the excess volume $V_0 = \partial G_0 / \partial p$, where $V_0 = \partial G_0 / \partial p$ and $S_0 = -\partial G_0 / \partial T$. The order parameter is zero for a simple fluid (which is described by a one-scale Gibbs energy) and changes from zero to unity as a function of p and T for a fluid with a two-scale nonideality of the Gibbs energy.

We also note that in the continuous (van der Waals like) scenario of liquid-liquid separation the function $f(\phi)$ is not symmetric with respect to the order parameter. Hence, the condition $h = h(T, p) = 0$ and the conditions of phase equilibrium (equal values of $h(T, p)$) are separated. In particular, for the given (van der Waals-like) example, the critical value of the order parameter $\phi_c = 1 / 3\tilde{b}$ and the critical temperature $T_c^* = 8\tilde{a} / 27k\tilde{b}$. However, in the vicinity of the critical point of phase separation the function $f(\phi)$ can be symmetrized by an appropriate redefinition of the order parameter ordering field [79].

III. DISCUSSION

a. Is the “critical-point-free” scenario realistic for supercooled water?

One result, reported in Section 6, has immediate practical implications. There is an ongoing discussion in the scientific community on the possibility of a “critical-point-free” scenario in silica and supercooled water, in which the first-order liquid-liquid phase transition continues into the stretched liquid state (doubly metastable), crossing the vapor-liquid spinodal [69, 67, 80-82]. This scenario is illustrated in Figure 4d. We conclude that this scenario is highly implausible for real water because it requires the disappearance of the locus of density maxima, collapsing into the transition line at negative pressures. In contrast, the locus of density maxima for real water is observed experimentally at positive pressures. This behavior of the density maxima is generic,

being reproduced for both the van der Waals model for state A and different forms of $G_{\text{BA}}(p, T)$ (see the Supplemental Material, figures S9d and S10).

b. Is Landau theory sufficient to unify different polyamorphic phenomena?

In this work we argue that the phenomenon of fluid polyamorphism can be unified by Landau theory of phase transitions. Landau theory is a mean-field approximation that neglects the effects of fluctuations on thermodynamic properties [37, 83]. However, these effects are significant only in the vicinity of the fluid-fluid critical points and second-order phase transitions and they do not qualitatively change the phase diagrams. Furthermore, the fluctuation effects are insignificant for first-order transitions and near tricritical points [69, 77, 83]. Effects of fluctuations can be incorporated into the two-state thermodynamics through a well-developed crossover procedure as described in ref. [84]. In other words, Landau theory is sufficient to address all basic issues of polyamorphic fluid phase behavior. Depending on the symmetry of the order parameter, fluid polyamorphism may or may not be accompanied by phase separation. If the order parameter is a scalar, the first-order transition between fluid phases may be terminated by a critical point. If the order parameter is a vector, a second-order transition without phase separation is possible. Moreover, coupling between scalar and vector order parameters may cause tricriticality and phase separation in a polyamorphic single-component fluid.

c. Can one discriminate, experimentally or computationally, between the “discrete” and “continuous” approaches to fluid polyamorphism?

While the symmetry of the order parameter (scalar vs. vector) can be elucidated by the study of polyamorphic phase behavior, discrimination between two alternative approaches (continuous vs. discrete) to fluid polyamorphism associated with a scalar order parameter, is a more delicate task. For the description of liquid-liquid transitions without well-defined discrete molecular states the difference between these approaches is somewhat similar to that between the descriptions of vapor-liquid transition either by the lattice-gas model or van der Waals model. In the continuous case the function $f(\phi)$ does not contain the entropy of mixing of two alternative states. Instead,

this function may have a form similar to the asymmetric van der Waals-like free energy. However, the difference between the vapor-liquid transitions in the symmetric lattice-gas model and asymmetric van der Waals model is subtle. Moghaddam et al. [57] developed a “fine lattice discretization” crossover procedure that uniformly describes these two models (see the Supplemental Material, Section 2). Similarly, the alternative formulations of the origin of liquid-liquid separation in a pure fluid, namely the existence of two interconvertible states or the existence of additional interaction energy/distance scales in the intermolecular potential, may generate very similar phase diagrams and indistinguishable thermodynamic anomalies. Moreover, both approaches, discrete and continuous, may generate similar extrema lines in the singularity-free scenario ($T_{c2} = 0$). For example, Poole et al. [80] proposed an extension of the van der Waals equation which incorporates the effects of the network of hydrogen bonds that exist in liquid water. This extension did not use the concept of the chemical reaction equilibrium between the two alternative structures and the entropy does not contain the entropy of mixing. The question arises: can these alternative approaches be discriminated either experimentally or computationally? Of course, the discrete approach to describe fluid polyamorphism is obviously applicable for polyamorphism caused by a well-defined chemical reaction (hydrogen, sulfur). Depending on the stoichiometric coefficients, the entropy of mixing may or may not have a symmetric form. For polyamorphism caused by polymerization the entropy of mixing the alternative states is extremely asymmetric (Eq. 18). In the case of $N \rightarrow \infty$ the extreme of the entropy of mixing fundamentally transforms the nature of the order parameter causing a lambda transition: entropy-driven polyamorphism without phase separation. A hypothetical example of a discrete, two-state approach with the perfectly symmetric entropy of mixing is equilibrium folding-unfolding of a single molecule. If the conformers of this molecule dislike each other, at certain temperature they may separate. For other debated examples of polyamorphism, including metastable liquid water, the question of the existence of two discrete states can only be answered if thermodynamic analysis is combined with dynamic and structural studies.

One of the arguments in favor of the discrete approach is the direct computation of the equilibrium number of molecules involved in alternative states in several simulated water-like models. The fractions of molecules involved in the high-density structure and in the low-density structure at various temperatures and pressures have been computed for the ST2 [45], TIP4P/2005 [85] and mW [86] models. Being well described by the two-state thermodynamics, the mW model

does not even exhibit liquid-liquid separation, behaving similar to the singularity-free scenario. We note that more accurate atomistic models of water are available for bulk properties [87], which have not yet been applied to this problem. In particular, the role of polarization is being increasingly recognized as having a significant influence on the properties of water [88, 89] and has not been considered so far.

The existence of a bimodal distribution of molecular configurations in real water is supported by X-ray absorption and emission spectroscopy [90], and by an investigation of vibrational dynamics [91]. An outstanding theoretical problem is a microscopic nature of the phenomenological order parameter (the molecular fraction of conversion in the two-state thermodynamics) associated with the bimodal distribution in supercooled water. The concept of locally favored structures, developed by Tanaka et al. [48-51] and account for coupling between the orientational and translational orders are promising steps in resolving this problem.

One unexplored area in both experiments and simulations is kinetics of interconversion of the alternative structures. The chemical-reaction approach to polyamorphism assumes that the chemical equilibrium is being established very fast, during picoseconds. The rate of the structural interconversion is to be tested by simulations and experimentally. In principle, the chemical relaxation rate can become slower upon cooling and may interplay with the rate of phase transformations.

Another outstanding question is the relation between the developed phenomenology of discrete alternative states and a two-scale isotropic intermolecular potential, such as the Jagla potential [92-95] or, more generally, soft-repulsion potentials [96, 97] that generate a liquid-liquid transition in a single-component system. As pointed out by Vilaseca and Franzese [96], isotropic intermolecular potentials, due to the lack of directional interactions, provide a mechanism for fluid polyamorphism that is an alternative to the bonding in network-forming liquids, such as water. It seems that the entropy of the systems described by an isotropic intermolecular potential may not contain the term that is associated with the entropy of mixing of two discrete states. However, how can the molecular clustering observed in simulations of a Jagla-potential fluid [98] be interpreted? In the discrete lattice-gas model there is no distance-dependent intermolecular potential. The discrete lattice-gas model and continuous van der Waals model can be reconciled by a crossover procedure known as the “fine lattice discretization” [57]. How could this procedure affect the evolution of the shape of intermolecular potential? Ultimately, any peculiarities in the condensed-

matter behavior are determined by details in interatomic and intermolecular interactions. Answers to the questions raised are highly desirable and require further investigation.

IV. CONCLUSIONS

Fluid polyamorphism is a surprisingly ubiquitous, yet poorly understood, phenomenon in condensed matter, either observed or predicted in a broad range of materials. We have developed a generic phenomenological approach, based on Landau theory of phase transitions, to describe polyamorphism in a single-component fluid. It is completely independent of the underlying molecular origin of the phenomenon and sheds new light on the physical nature of polyamorphism.

We utilized the concept of thermodynamic equilibrium between two competing interconvertible states or molecular structures. The existence of two competing states in a single-component fluid may promote fluid polyamorphism either with or without phase separation depending on the nature of the order parameter. If the order parameter is a scalar, associated with the molecular fraction of conversion, the polyamorphism is accompanied by fluid phase separation. If the order parameter is a vector (lambda transition in helium, polymerization in the limit $N \rightarrow \infty$), the polyamorphism may be accompanied by phase separation only at the account for coupling of the vector order parameter with a scalar order parameter, causing tricriticality.

The two-state thermodynamics naturally unifies all the debated cases of fluid polyamorphism: with and without phase separation, from the “singularity-free” scenario to the “critical-point-free” one and qualitatively describes the thermodynamic anomalies typically observed in polyamorphic materials. Significantly, we can conclude that the critical-point-free scenario in supercooled water (with the liquid-liquid transition line crossing the vapor-liquid spinodal) is highly unlikely. We have found a remarkable peculiarity of liquid polyamorphism, which has not been reported previously in the literature, a singularity (“bird’s beak”) in the liquid-liquid coexistence curve when the critical point coincides with the liquid-vapor spinodal. This singularity is associated with the common tangent of the liquid-liquid coexistence and vapor-liquid spinodal.

The developed approach enables a global equation of state to be formulated that generically describes both vapor-liquid and liquid-liquid equilibria in single-component fluids, including the metastable states under negative pressures. Further experimental and simulation studies of dynamic

and structural properties are desirable to verify other predictions of this approach and elucidate the microscopic foundation of the developed phenomenology.

ACKNOWLEDGEMENTS

We acknowledge fruitful discussions with S. V. Buldyrev, P. G. Debenedetti, M. E. Fisher, G. Franseze, J. Hrubý, P. Poole, H. E. Stanley, and J. V. Sengers. Mikhail Anisimov thanks Swinburne University of Technology, Australia for funding under the auspices of the Distinguished Visiting Researcher Scheme, the Institute of Multiscale Science and Technology (Labex iMUST) supported by the French ANR, and by the Russian Foundation for Basic Research (Grant No. 16-03-00895-a) during part of his sabbatical leave from the University of Maryland. The research of Michal Duška at the University of Maryland was supported by the Young Scientist IAPWS Fellowship Project “Towards an IAPWS Guideline for the Thermodynamic Properties of Supercooled Heavy Water”.

1. A. Ha, I. Cohen, X. L. Zhao, M. Lee M and D. Kivelson, *Supercooled liquids and polyamorphism*, J. Phys. Chem. **100**, 1 (1996).
2. P. H. Poole, T. Grand, C. A. Angell and P. F. McMillan, *Polymorphic phase transitions in liquids and glasses*, Science **275**, 322 (1997).
3. G. Franzese, G. Malescio, A. Skibinsky, S. V. Buldyrev and H. E. Stanley, *Generic mechanism for generating a liquid–liquid phase transition*, Nature **409**, 692 (2001).
4. H. E. Stanley (editor), *Liquid Polymorphism*, Advances in Chemical Physics, (John Wiley & Sons, 2013), Vol 152.
5. F. Sciortino, *Liquid-liquid transitions: Silicon in silico*, Nature Physics **7**, (2011).
6. A. Schmitt, *Introduction to Superfluidity*, Lecture Notes in Physics (Springer International Publishing, 2015), Vol 888, p. 1.
7. D. Vollhardt and P. Wölfle, *The Superfluid Phases of Helium 3* (Taylor and Francis, London, 1990).
8. A. V. Tobolsky and A. Eisenberg, *Equilibrium polymerization of sulfur*, J. Am. Chem. Soc. **81**, 780 (1959).
9. R. Bellissent, L. Descotes and P. Pfeuty, *Polymerization in liquid sulphur*, J. Phys.-Cond. Matt. **6**, A211 (1994).

10. V. F. Kozhevnikov, W. B. Payne, J. K. Olson, C. L. McDonald and C. E. Inglefield, *Physical properties of sulfur near the polymerization transition*, J. Chem. Phys. **121**, 7379 (2004).
11. Y. Katayama, T. Mizutani, W. Utsumi, O. Shimomura, M. Yamakata, and K. Funakoshi, *A first-order liquid-liquid phase transition in phosphorus*, Nature **403**, 170 (2000).
12. J. N. Glosli and F. H. Ree, *Liquid-liquid phase transformation in carbon*, Phys. Rev. Lett. **82**, 4659 (1999).
13. A. Cadien, Q. Y. Hu, Y. Meng, Y. Q. Cheng, M. W. Chen, J. F. Shu, H. K. Mao and H. W. Sheng, *First-order liquid-liquid phase transition in cerium*, Phys. Rev. Lett. **110**, 125503 (2013).
14. L. I. Aptekar, *Phase transitions in non-crystalline germanium and silicon*, Sov. Phys. Doklady **24**, 993 (1979).
15. S. Sastry and C. A. Angell, *Liquid-liquid phase transition in supercooled silicon*, Nature Materials **2**, 739 (2003).
16. M. Beye, F. Sorgenfrei, W. F. Schlotter, W. Wurth and A. Föhlisch, *The liquid-liquid phase transition in silicon revealed by snapshots of valence electrons*, Proc. Natl. Acad. Sci. USA **107**, 16772 (2010).
17. V. V. Vasisht, S. Saw and S. Sastry, *Liquid-liquid critical point in supercooled silicon*, Nature Phys. **7**, 549 (2011).
18. I. Saika-Voivod, F. Sciortino and P. H. Poole, *Computer simulations of liquid silica: Equation of state and liquid-liquid phase transition*, Phys. Rev. E. **63**, 011202 (2000).
19. D. J. Lacks, *First-order amorphous-amorphous transformation in silica*, Phys. Rev. Lett. **84**, 4629 (2000).
20. E. Lascaris, *Tunable liquid-liquid critical point in an ionic model of silica*, Phys. Rev. Lett. **116**, 125701 (2016).
21. Y. Tsuchiya and E. F. W. Seymour, *Thermodynamic properties of the selenium-tellurium system*, J. Phys. C: Solid State Phys. **15**, L687 (1982).
22. Y. Tsuchiya and E. F. W. Seymour, *Thermodynamic properties and structural inhomogeneity of liquid tellurium*, J. Phys. C: Solid State Physics **18**, 4721 (1985).
23. Y. Tsuchiya, *Thermodynamic evidence for a structural transition of liquid Te in the supercooled region*, J. Phys.: Condens. Matter **3**, 3163 (1991).
24. K. Fuchizaki, T. Hase, A. Yamada, N. Hamaya, Y. Katayama, and K. Funakoshi, *Polyamorphism in tin tetraiodide*, J. Chem. Phys. **130**, 121101 (2009).
25. K. Fuchizaki, N. Hamaya, T. Hase, and Y. Katayama, *Communication: Probable scenario of the liquid-liquid phase transition of SnI₄*, J. Chem. Phys. **135**, 091101 (2011).
26. M. A. Morales, C. Pierleoni, E. Schwegler and D. M. Ceperley, *Evidence for a first-order liquid-liquid transition in high-pressure hydrogen from ab initio simulations*, Proc. Natl. Acad. Sci. USA **107**, 12799 (2010).
27. M. Zaghoo, A. Salamat, and I. F. Silvera, *Evidence of a first-order phase transition to m hydrogen*, Phys. Rev. B **93**, 155128 (2016).
28. P. Dalladay-Simpson, R. T. Howie, and E. Gregoryanz, *Evidence for a new phase of dense hydrogen above 325 gigapascals*, Nature **529**, 63 (2016).
29. P. H. Poole, F. Sciortino, U. Essman and H. E. Stanley, *Phase behavior of metastable water*, Nature **360**, 324 (1992).

30. M. C. Bellissent-Funel, *Is there a liquid-liquid phase transition in supercooled water?* Europhys. Lett. **42**, 161 (1988).
31. O. Mishima and H. E. Stanley, *Decompression-induced melting of ice IV and the liquid-liquid transition in water*, Nature **392**, 164 (1988).
32. Debenedetti PG (1998) *Condensed matter: One substance, two liquids?* Nature 392: 127-128.
33. O. Mishima and H. E. Stanley, *The relationship between liquid, supercooled and glassy water*, Nature **396**, 329 (1988).
34. P. Gallo, K. Amann-Winkel, C. A. Angell, M. A. Anisimov, F. Caupin, C. Chakravarty, E. Lascaris, T. Loerting, A. Z. Panagiotopoulos, R. J. Sellberg, H. E. Stanley, H. Tanaka, C. Vega, L. Xu, and L. G. M. Pettersson, *Water: A tale of two liquids*, Chem. Rev. **116**: 7463-7500 (2016).
35. F. Caupin. *Escaping the no man's land: Recent experiments on metastable liquid water*, J. Non Cryst.. Sol., **407**, 441-448 (2015).
36. J. C. Palmer, F. Martelli, Y. Liu, R. Car, A. Z. Panagiotopoulos, and P. G. Debenedetti, *Metastable liquid-liquid transition in a molecular model of water*, Nature **510**, 385 (2014); *Reply to D. Chandler*, Nature **531**, E2 (2014).
37. L. D. Landau and E. M. Lifshitz, *Statistical Physics, Part I*, 3rd Ed. (Butterworth Heinemann, Oxford, 1980).
38. H. Whiting, *A new theory of cohesion applied to the thermodynamics of liquids and solids*, Proc. Am. Acad. Arts Sci. **19**, 353 (1884).
39. W. C. Röntgen, *Ueber die Constitution des flüssigen Wassers*, Ann. Phys. (Leipzig) **281**, 91, (1892).
40. E. Rapoport, *Model for melting curve maxima at high pressure*, J. Chem. Phys. **46**, 2891 (1967).
41. S. Sastry, F. Sciortino F, and H. E. Stanley, *Limits of stability of the liquid phase in a lattice model with water-like properties*, J. Chem. Phys. **98**, 9863 (1993).
42. C. T. Moynihan, *Two species nonideal solution model for amorphous phase transitions*, Mater Res. Soc. Con. Proc. **455**: 411 (1997).
43. E. G. Ponyatovsk, V. V. Sinitsyn, and T. A. Pozdnyakova, *The metastable T-PT-P phase diagram and anomalous thermodynamic properties of supercooled water*, J. Chem. Phys. **109**, 2413 (1998).
44. A. Ciach, W. Gózdź, and A. Perera, *Simple three-state lattice model for liquid water*. Phys. Rev. E **78**, 021203(2008).
45. M. J. Cuthbertson and P. H. Poole, *Mixture-like behavior near a liquid-liquid phase transition in simulations of supercooled water*, Phys. Rev. Lett. **106**, 115706 (2011).
46. C. E. Bertrand and M. A. Anisimov, *Peculiar thermodynamics of the second critical point in supercooled water*, J. Phys. Chem. B **115**, 14099 (2011).
47. V. Holten and M. A. Anisimov, *Entropy driven liquid-liquid separation in supercooled water*, Sci. Rep. **2**, 713 (2012).
48. H. Tanaka, *Simple physical model of liquid water*, J. Chem. Phys. **112**, 799 (2000).

49. H. Tanaka, *Bond orientational order in liquids: Towards a unified description of water-like anomalies, liquid-liquid transition, glass transition, and crystallization*, Eur. Phys. J. E **35**, 113 (2012).
50. H. Tanaka, *Importance of many-body orientational correlations in the physical description of liquids*, Faraday Discuss **167**, 9 (2013).
51. J. Russo and H. Tanaka, *Understanding water's anomalies with locally favored structures*, Nature Commun. **5**, 3556 (2014).
52. Q. Zheng, D. J. Durben, G. H. Wolf, and C. A. Angell, *Liquids at large negative pressures: Water at the homogeneous nucleation limit*, Science **254** (5033) 829–832 (1991).
53. M. El Mekki Azouzi, C. Ramboz, J.-F. Lenain, and F. Caupin, *A coherent picture for water at extreme negative pressure*, Nature Phys. **38**-41 (2013).
54. G. Pallares, M.A. Gonzalez, J.L.F. Abascal, C. Valeriani and F. Caupin. *Equation of state for water and its line of density maxima down to 120 MPa*, Phys. Chem. Chem. Phys. **18**, 5896-5900 (2016).
55. I. Prigogine and R. Defay, *Chemical Thermodynamics* (Longmans, Green & Co., London, 1954).
56. R. Kubo, *Statistical Mechanics* (Elsevier, Amsterdam, 1965).
57. S. Moghaddam, Y. C. Kim, and M. E. Fisher, *Convergence of fine-lattice discretization for near-critical fluids*, J. Phys. Chem. B **109**, 6824 (2005).
58. K. Stokely, M. G. Mazza, H. E. Stanle and G. Franzese, *Effect of hydrogen bond cooperativity on the behavior of water*, Proc. Natl. Acad. Sci. USA **107**: 1301 (2010).
59. S. Sastry, P. G. Debenedetti, F. Sciortino, and H. E. Stanley, *Singularity-free interpretation of the thermodynamics of supercooled water*, Phys. Rev. E **53**, 6144–6154 (1996).
60. (a) F. Sciortino, P. H. Poole, U. Essmann and H. E. Stanley, *Line of compressibility maxima in the phase diagram of supercooled water*, Phys. Rev. E **55**, 727 (1997). (b) P.H. Poole, I. Saika-Voivod and F. Sciortino, *Density minimum and liquid-liquid phase transition*, J. Phys.-Cond. Matt. **17**, L431 (2005)
61. V. Holten, C. Qiu, E. Guillermin, M. Wilke, J. Ricka, M. Frenz, and F. Caupin, *Compressibility anomalies in stretched water and their interplay with density anomalies*, arXiv:1708.00063 [physics.chem-ph].
62. D. Dhabal, C. Chakravarty, V. Molinero and N. K. Kashyap, *Comparison of liquid-state anomalies in Stillinger-Weber models of water, silicon, and germanium*, J. Chem. Phys. **145**, 214502 (2016).
63. V. Holten, D. T. Limmer, V. Molinero and M. A. Anisimov, *Nature of the anomalies in the supercooled liquid state of the mW model of water*, J. Chem. Phys. **138**, 174501 (2013).
64. M. A. González, C. Valeriani, F. Caupin, and J. L. F. Abascal, *A Comprehensive scenario of the thermodynamic anomalies of water using the TIP4P/2005 model*, J. Chem. Phys. **145**, 054505 (2016).
65. J. W. Biddle, R. S. Singh, E. M. Sparano, F. Ricci, M. A. González, C. Valeriani, J. L. F. Abascal, P. G. Debenedetti, M. A. Anisimov, and F. Caupin, *Two-structure thermodynamics for the TIP4P/2005 model of water covering supercooled and deeply stretched regions*, J. Chem. Phys. **146**: 034502 (2017).

66. M. G. Mazza, K. Stokely, H. E. Stanley, and G. Franzese, *Effect of pressure on the anomalous response functions of a confined water monolayer at low temperature*, J. Chem. Phys. **137**, 204502 (2012).
67. R. Chen, E. Lascaris and J. C. Palmer, *Liquid-liquid phase transition in an ionic model of Silica*, J. Chem. Phys. **146**, 234503 (2017).
68. J. M. H. Levelt Sengers, *Solubility near the solvent's critical point*, J. Supercrit. Fluids **4**, 215 (1991).
69. I. D. Lawrie and S. Sarbach, *Theory of tricritical points in Phase Transitions and Critical Phenomena*, edited by C. Domb and J. L. Lebowitz (Academic Press, New York, 1984), Vol. 9, p. 163.
70. M. A. Anisimov, *Critical Phenomena in Liquids and Liquid Crystals* (Gordon & Breach, Reading, 1991).
71. J. C. Wheeler, S. J. Kennedy and P. Pfeuty, *Equilibrium polymerization as a critical phenomenon*, Phys. Rev. Lett. **45**, 1748 (1980).
72. J. C. Wheeler and P. Pfeuty, *The $n \rightarrow 0$ Vector model and equilibrium polymerization*, Phys. Rev. A **24**, 1050 (1981).
73. J. Dudowicz and K. F. Freed and J. F. Douglas, *Lattice model of living polymerization. I: Basic Thermodynamic Properties*, J. Chem. Phys. **111**, 7116 (1999); *Lattice model of living polymerization. II: Interplay between polymerization and phase stability*, J. Chem Phys. **112**, 1002 (2000); *Lattice model of living polymerization. III: Evidence for particle clustering from phase separation properties and "rounding" of the dynamical clustering transition*, J. Chem. Phys **113**, 434 (2000).
74. P. J. Flory, *Thermodynamics of high polymer solutions*, J. Chem. Phys. **10**, 51 (1942). P. J. Flory, *Principles of Polymer Chemistry* (Cornell University, Ithaca, NY, 1953).
75. P.-G. de Gennes, *Scaling Concepts in Polymer Physics* (Cornell University Press, Ithaca, NY, 1979).
76. M. E. Fisher, *The story of coulombic criticality*, J. Stat. Phys, **75**, 1-36 (1994).
77. J. S. Hager, M. A. Anisimov, and J. V. Sengers, *Scaling of demixing curves and crossover from critical to tricritical behavior in polymer solutions*, J. Chem. Phys. **117**, 5940-5950 (2002).
78. J. C. Wheeler, *Symmetric and nonsymmetric tricritical points in liquid sulfur and "living polymer" solutions*, J. Chem. Phys. **81**, 3635 (1984).
79. C. E. Bertrand, J. F. Nicoll, and M. A. Anisimov, *Comparison of complete scaling and a field-theoretic treatment of asymmetric fluid criticality*, Phys. Rev. E **85**, 031131 (2012).
80. P. H. Poole, F. Sciortino, T. Grande, H. E. Stanley, and C. A. Angell, *Effect of hydrogen bonds on the thermodynamic behavior of liquid water*, Phys. Rev. Lett **73**, 1632 (1994).
81. C. A. Angell and V. Kapko, *Potential Tuning in the SW system. (I) Bringing $T_{c,2}$ to Ambient Pressure, and (II) Colliding $T_{c,2}$ with the Liquid Vapor Spinodal*, J. Stat. Mech: Theory & Exp., Special issue on structure in glassy and jammed systems, 094004 (2016).
82. G. Pallares, M. E. M. Azouzi, M. A. González, J. L. Aragonés, J. L. F. Abascal, C. Valeriani, and F. Caupin, *Anomalies in bulk supercooled water at negative pressure*, Proc. Natl. Acad. Sci. USA **111**, 7936 (2014).

83. M. E. Fisher, in *Lecture Notes in Physics*, edited by F. J. W. Hahne Springer, Berlin, 1982, Vol. 186, p. 1.
84. V. Holten, J. C. Palmer, P. H. Poole, P. G. Debenedetti, and M. A. Anisimov, *Two-State Thermodynamics of the ST2 Model for Supercooled Water*, J. Chem. Phys. **140**, 104502 (2014).
85. R. S. Singh, J. W. Biddle, P. G. Debenedetti, M. A. Anisimov, *Two-state thermodynamics and the possibility of a liquid-liquid phase transition in supercooled TIP4P/2005*, J. Chem. Phys. **144**, 144504 (2016)
86. V. Molinero and E. B. Moore, *Growing correlation length in supercooled water*, J. Chem. Phys. **130**, 244505 (2009).
87. I. Shvab and R. J. Sadus, *Atomistic water models: Aqueous thermodynamic properties from ambient to supercritical conditions*, Fluid Phase Equilib. **407**, 6 (2016).
88. T. M. Yigzawe and R. J. Sadus, *Thermodynamic properties of liquid water from a polarizable intermolecular potential*, J. Chem. Phys. **138**, 044503 (2013).
89. I. Shvab and R. J. Sadus, *Intermolecular potentials and the accurate predication of the thermodynamic properties of water*, J. Chem. Phys. **139**, 194505 (2013).
90. F. Perakis, K. Amann-Winkel, F. Lehmkuhler, M. Sprung, D. Mariedahl, J. A. Sellberg, H. Pathak, A. Späh, F. Cavalca, D. Schlesinger, A. Ricci, A. Jain, B. Massani, F. Aubree, C. J. Benmore, T. Loerting, G. Grübel, L. G. M. Pettersson, and A. Nilsson A, *Diffusive dynamics during the high-to-low density transition in amorphous ice*. Proc. Natl. Acad. Sci. USA, DOI: 10.1073/pnas.1705303114 (2017).
91. A. Taschin, P. Bartolini, R. Eramo, R. Righini, and R. Torre, *Evidence of two distinct local structures of water from ambient to supercooled conditions*, Nature Commun 4, 2401 (2013).
92. E. A. Jagla, *Liquid-liquid equilibrium for monodisperse spherical particles*, Phys. Rev. E **63**, 061501 (2001).
93. G. Malescio, G. Franzese, A. Skibinsky, S. V. Buldyrev, and H. E. Stanley, *Liquid-liquid phase transition for an attractive isotropic potential with wide repulsive range*, Phys. Rev. E **71**, 061504 (2005).
94. N. M. Barraza, E. Salcedo, and M. C. Barbosa, *Thermodynamic, Dynamic and Structural Anomalies for Shoulder-Like Potentials*, J. Chem. Phys., **131**, 094504 (2009).
95. F. Ricci, and P. G. Debenedetti, *A free energy study of the liquid-liquid phase transition of the Jagla two-scale potential*, J. Chem. Sci. **129**, 801 (2017).
96. P. Vilaseca and G. Franzese, *Isotropic soft-core potentials with two characteristic length scales and anomalous behavior*, J. Non-Crystall. Solids **357**, 419–426 (2011).
97. Yu. D. Fomin, E. N. Tsiok, and V. N. Ryzhov, *Silicalike sequence of anomalies in core-softened systems*, Phys. Rev. E **87**, 042122 (2013).
98. L. Xu, I. Ehrenberg, S. V. Buldyrev and H. E. Stanley, *Relationship between the liquid–liquid phase transition and dynamic behaviour in the Jagla model*, J. Phys.-Cond. Matt. **8**, S2239 (2006).

Thermodynamics of Fluid Polyamorphism

Mikhail A. Anisimov^{1,2*}, Michal Duška^{1,3}, Frédéric Caupin⁴, Lauren E. Amrhein¹,

Amanda Rosenbaum¹, and Richard J. Sadus⁵

¹*Department of Chemical & Biomolecular Engineering and Institute for Physical Science & Technology,
University of Maryland, College Park, U.S.A.*

²*Oil and Gas Research Institute of the Russian Academy of Sciences, Moscow, 117333, Russia*

³*Institute of Thermomechanics, Academy of Sciences of the Czech Republic, 182 00 Prague 8, Czech
Republic*

⁴*Univ Lyon, Université Claude Bernard Lyon 1 & CNRS, Institut Lumière Matière, F-69622, Lyon, France*

⁵*Centre for Molecular Simulation, Swinburne University of Technology, Hawthorn, Victoria 3122,
Australia*

*To whom correspondence should be addressed. Email: anisimov@umd.edu.

SUPPLEMENTAL MATERIAL

1. Lattice-gas model

The lattice-gas model was first introduced by Frenkel in 1932 [1]. In 1952 Yang and Lee showed that the lattice-gas model, which is the simplest model for the vapor-liquid transition, is mathematically equivalent to the Ising model that describes a phase transition between paramagnetic and anisotropic ferromagnetic or antiferromagnetic states. The Ising/lattice-gas model is also used to describe solid-solid phase separation or order-disorder transitions in binary alloys as well as liquid-liquid phase separation in binary fluids. The model plays a special role in the physics of condensed matter because it can be applied to very different systems and phenomena, thereby bridging the gap between the physics of fluids and solid-state physics [3-5]. The volume of the system is divided into cells of molecular size l_0 . These cells are arranged in a lattice with the coordination number z ($z = 6$ for a simple cubic lattice). In its simplest version each cell in the lattice is either empty or occupied by only one molecule. The molecular density in the

lattice gas model is dimensionless, being defined as $\rho = l_o^3 (N/V)$, where N is the number of occupied cells. The nearest-neighboring molecules interact by short-ranged attractive forces. Empty cells do not interact with their neighbors.

The exact analytical solution for the three-dimensional lattice gas has not been so far obtained, though rather accurate numerical solutions are available. The simplest approximate analytical solution can be obtained in the mean-field approximation, with the multi-body attraction energy being represented by a single interaction parameter ε . This approximation is equivalent to accounting for attraction in the van der Waals fluid via the constant a . Similarly, the molecular volume of the lattice gas (l_o^3) is equivalent to the van der Waals co-volume parameter (b).

The equation of state for lattice gas in the mean-field approximation reads

$$p = -k_B T \ln(1 - \rho) - \varepsilon \rho^2, \quad (\text{S1})$$

where p , T , and k_B are the pressure, temperature and Boltzmann constant, respectively. In Eq (S1), the pressure is in units of energy and the density is dimensionless. The chemical potential μ of the lattice gas and the density of the Helmholtz energy $\rho F = \rho\mu - p$ in the mean-field approximation are

$$\mu = \left[\frac{\partial(\rho F)}{\partial \rho} \right]_T = k_B T \ln \frac{\rho}{1 - \rho} - 2\varepsilon \rho + \varepsilon + \varphi(T) \quad (\text{S2})$$

and

$$\rho F = \rho\mu - p = k_B T \rho \ln \rho + k_B T (1 - \rho) \ln(1 - \rho) + \varepsilon \rho(1 - \rho) + \rho \varphi(T). \quad (\text{S3})$$

The function $\varphi(T)$ represents the Helmholtz energy of ideal gas per molecule that depends on temperature only. This function does not affect the phase equilibrium but is needed to calculate the heat capacity.

After subtracting the terms linear in ρ , the Helmholtz energy obtained from Eq. (S3) is symmetric with respect to ρ . This means that, unlike that in the essentially asymmetric van der Waals fluid, the condition for fluid-phase equilibrium (binodal) for the lattice gas can be found analytically from

$$\mu_{\text{exc}} - \varphi(T) = k_B T \ln \frac{\rho}{1-\rho} - 2\varepsilon\rho + \varepsilon = 0. \quad (\text{S4})$$

The vapor-liquid spinodal

$$\left(\frac{\partial \mu}{\partial \rho} \right)_T = \frac{k_B T}{\rho(1-\rho)} - 2\varepsilon = 0 \quad (\text{S5})$$

The critical-point parameters are $\rho_c = 1/2$, $T_c = \varepsilon / 2k_B$, $p_c = k_B T_c [-\ln(1/2) - 1/2] \cong 0.193 k_B T_c$.

In the reduced form ($\hat{T} = T/T_c$, $\hat{p} = p_c$) the lattice-gas equation of state reads

$$\hat{p} = \frac{\hat{T} \ln(1-\rho) + 2\rho^2}{\ln \frac{1}{2} + \frac{1}{2}} \cong -5.18 [\hat{T} \ln(1-\rho) + 2\rho^2]. \quad (\text{S6})$$

The critical-point parameters are $\rho_c = 1/2$, $\hat{T}_c = 1$, and $\hat{p}_c = 1$.

The equation for spinodal reads

$$\hat{T}_{\text{sp}} = 4\rho(1-\rho). \quad (\text{S7})$$

The liquid-vapor coexistence

$$\frac{1}{\hat{T}_{\text{exc}}} = \frac{\frac{1}{2} \ln \frac{\rho}{1-\rho}}{2\rho - 1}. \quad (\text{S8})$$

The lattice-gas model mathematically equivalent to the Ising model of an incompressible anisotropic ferromagnetic material. In zero magnetic field, the magnetization, M , spontaneously emerges at a certain temperature i.e., the ‘‘Curie temperature’’. Introducing $M = 2\rho - 1$ and using

the mathematical fact that $\text{arctanh}(M) = \frac{1}{2} \ln \frac{1+M}{1-M}$, we obtain $\frac{M}{\hat{T}_{\text{exc}}} = \frac{1}{2} \ln \frac{1+M}{1-M}$. Hence,

$$M = \tanh \frac{M}{\hat{T}_{\text{exc}}}. \quad (\text{S9})$$

Equation (9) is commonly used for the Ising model, describing the spontaneous magnetization below the Curie point of a ferromagnetic-paramagnetic transition.

Figures S1 and S2 demonstrate the phase behavior and properties of the lattice-gas model.

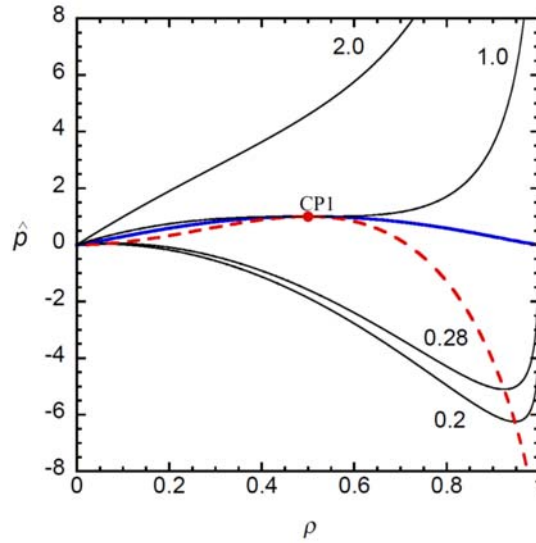


Fig. S1. Selected isotherms and liquid-vapor coexistence of the lattice-gas model. Solid blue is binodal. Dashed red is spinodal. Red dot is the liquid-vapor critical point.

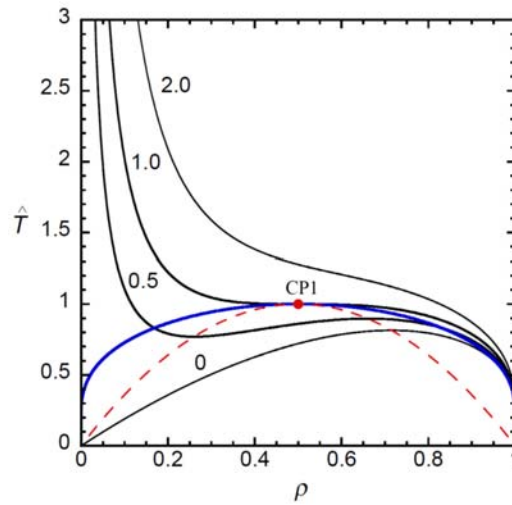


Fig. 2. Selected isobars and liquid-vapor coexistence of the lattice-gas model. Solid blue is binodal. Dashed red is spinodal. Red dot is the liquid-vapor critical point.

2. “Fine lattice discretization”: crossover between lattice gas and van der Waals fluid

Moghaddam et al. [6] developed a procedure, “fine lattice discretization”, describing crossover between two limits: the discrete, lattice-gas model and the continuous, van der Waals model. Helmholtz energy per unit volume and chemical potential for lattice gas:

$$\rho F = \rho\mu - p = kT\rho \ln \rho + kT(1-\rho) \ln(1-\rho) + \varepsilon\rho(1-\rho) + \rho\varphi(T). \quad (\text{S10})$$

$$\mu = \left[\frac{\partial(\rho F)}{\partial \rho} \right]_T = kT \ln \frac{\rho}{1-\rho} - 2\varepsilon\rho + \varphi(T). \quad (\text{S11})$$

$$\mu_{\text{cxc}} - \mu_0(T) = kT \ln \frac{\rho}{1-\rho} - 2\varepsilon\rho = 0. \quad (\text{S12})$$

For the van der Waals fluid, the density of the Helmholtz energy is

$$\rho F = kT\rho \ln \frac{\rho}{1-\rho} - \varepsilon\rho^2 + \rho\varphi(T) \quad (\text{S13})$$

In Eq. (S13) we use the following rescaling of the physical density and the van der Waals parameter a : $\rho \rightarrow b\rho$ and $a \rightarrow \varepsilon = a/b$.

$$\mu = \left[\frac{\partial(\rho F)}{\partial \rho} \right]_T = kT \ln \frac{\rho}{1-\rho} + \frac{kT}{1-\rho} - 2\varepsilon\rho + \varphi(T). \quad (\text{S14})$$

$$\rho_c = \frac{1}{3}, \quad T_c = \frac{8\varepsilon}{27kb}. \quad (\text{S15})$$

Fine lattice discretization model:

$$\frac{\mu - \mu_0(T)}{kT} = \ln \frac{\rho}{1 + \rho(1/\zeta - 1)} + \zeta \ln \left(1 + \frac{\rho}{\zeta(1-\rho)} \right) - \frac{2a\rho}{kT}. \quad (\text{S16})$$

Discretization parameter $\zeta = l/l_0$ (l molecular diameter, l_0 lattice spacing)

$\zeta = 1 \rightarrow$ lattice gas

$\zeta \rightarrow \infty \rightarrow$ van der Waals fluid

$$\rho_c = \frac{1}{2}\psi_1(\zeta), \quad T_c = \frac{\varepsilon}{2k}\psi_2(\zeta).$$

The critical density and temperature are functions of the discretization parameter.

3. **Fluid polyamorphism caused by thermodynamic equilibrium between interconvertible states A and B: an alternative choice of the equilibrium constant as a function of temperature and pressure with the lattice-gas EOS for state A**

Consider an alternative choice of $\ln K(\hat{T}, \hat{p})$ for the “reaction” $A \rightleftharpoons B$ to be a linear function of temperature and pressure:

$$-\ln K(\hat{T}, \hat{p}) = \lambda'(\hat{T} + \alpha' \hat{p} + \beta'), \quad (\text{S17})$$

$$\hat{G}_{\text{BA}}(\hat{T}, \hat{p}) = -\hat{T} \ln K(\hat{T}, \hat{p}) = \lambda'(\hat{T}^2 + \alpha \hat{p} \hat{T} + \beta \hat{T}). \quad (\text{S18})$$

This choice corresponds to the changes in both reaction energy ($\hat{U}_{\text{BA}} = \lambda' \hat{T}^2$) and the volume ($\hat{V}_{\text{BA}} = \alpha' \hat{T}$) to vanish at zero temperature. The line $\hat{T} + \alpha' \hat{p} + \beta' = 0$ is the locus of liquid-liquid transitions. The $p-T$ and $T-\rho$ phase diagrams for a specific case with $\lambda' = 10$, $\alpha' = 0.02$, and $\beta' = -0.3$ is presented in Figs. S3 – S7. We observed that when the volume change of reaction vanishes at zero temperature, the density difference between the coexisting liquid phases also vanishes.

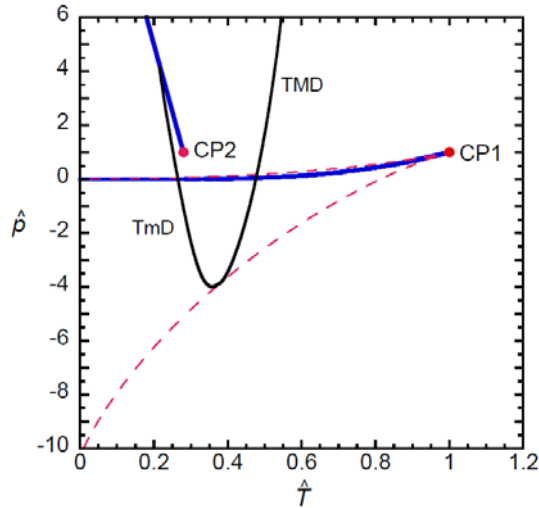


Fig. S3. P - T diagram of lattice gas with the second (liquid-liquid) transition. Two blue curves are vapor-liquid and liquid-liquid transitions terminated by the critical points CP1 and CP2 (shown by red dots), respectively. Solid black are the loci of minimum density (TmD) and maximum density (TMD). Dashed reds are two branches of the vapor-liquid spinodal. Thermodynamically, liquid can exist between the vapor-liquid coexistence and the low branch of spinodal as a metastable state.

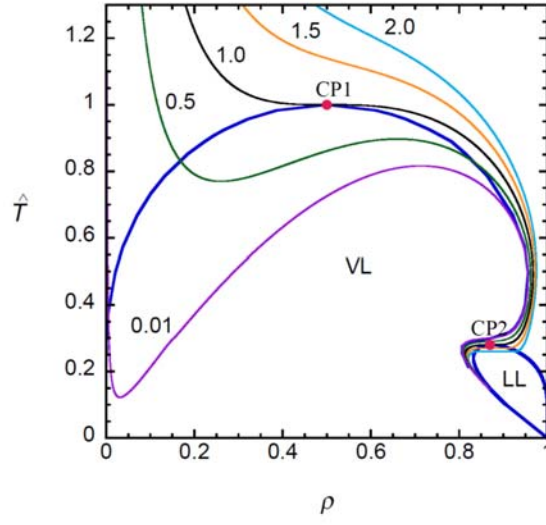


Fig. S4. Selected isobars, liquid-vapor (LV) and liquid-liquid (LL) coexistence (both shown by thick blue curves) of the lattice-gas model with “chemical reaction”. Solid blue curves are the binodals. Red dots are the liquid-gas and liquid-liquid critical points.

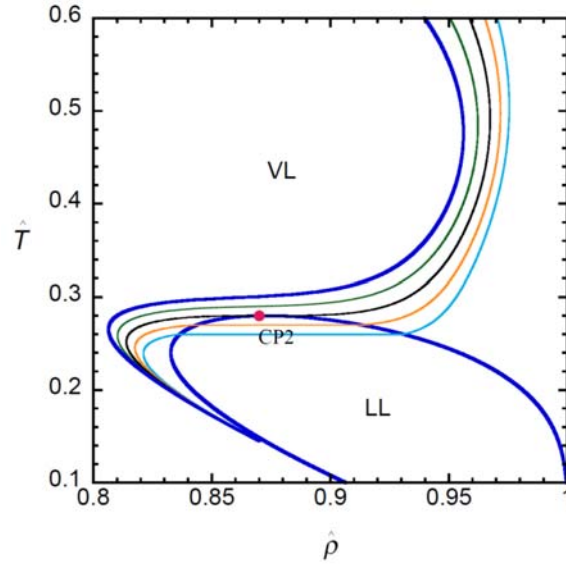


Fig. S5. Selected isobars in the vicinity of the liquid-liquid coexistence (shown by thick blue) of the lattice-gas model with “chemical reaction”.

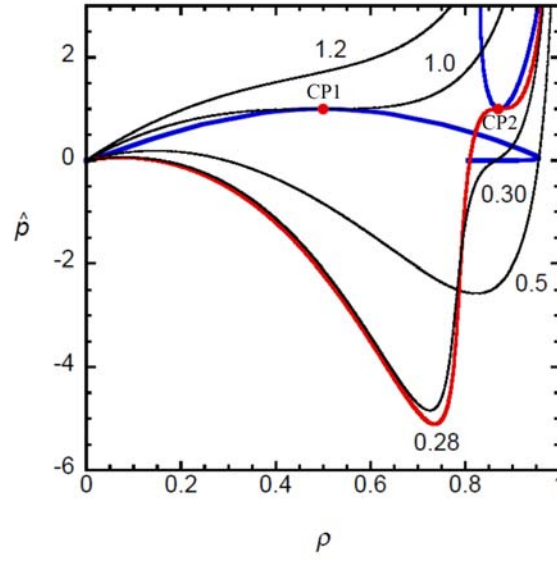


Fig. S6. Selected isotherms, liquid-vapor and liquid-liquid coexistence (both shown by thick blue curves) of the lattice-gas model with “chemical reaction”. Red curve is the critical isotherm of liquid-liquid coexistence. Red dots are the liquid-gas and liquid-liquid critical points.

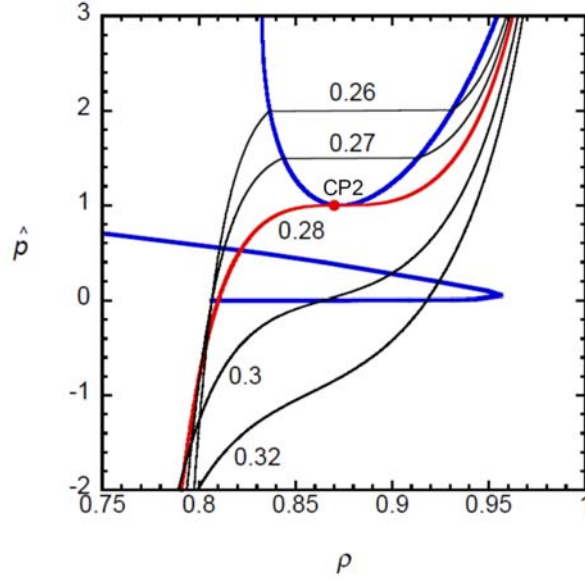


Fig. S7. Selected isotherms in the vicinity of the liquid-liquid coexistence (shown by thick blue) of the lattice-gas model with “chemical reaction”. Red curve is the critical isotherm of liquid-liquid coexistence. Red dot is the liquid-liquid critical point.

The fraction of state B as a function of temperature for selected isobars is presented in Fig. S8.

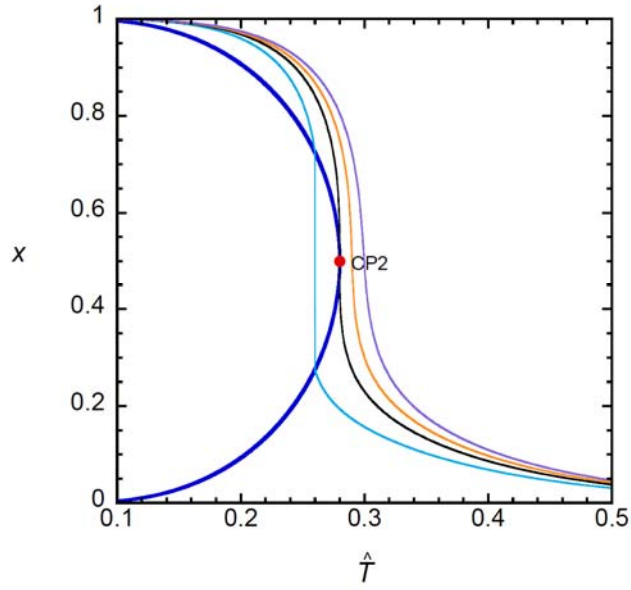


Fig. S8. Fraction of state B as a function of temperature for selected isobars (from left to right: $\hat{p} = 2.0, 1.0, 0.5$, and 0.01) and along the liquid-liquid coexistence ($\ln K(T, p) = 0$, thick blue). Red dot is the liquid-liquid critical point.

4. Fluid polyamorphism (the van der Waals equation as a choice for state A): tuning the location of the liquid-liquid critical point

The phase diagrams predicted by two-state thermodynamics, if the van der Waals model is chosen for state A, is essentially similar to those of the lattice-gas model for state A. The evolution of the extrema loci upon tuning the location of the liquid-liquid critical point is demonstrated in Figure S9 from (A) (singularity-free scenario) to (D) (critical point-free scenario). The disappearance of the maximum density locus in the case where the critical point coincides with the vapor-liquid spinodal point is demonstrated in Figure S10 by zooming (C). Figures S9 A to D show the extrema patterns similar to those in Figure 4 of the main text. The parameters of the liquid-liquid transition/Widom line, as defined by Eq. (15) of the main text, in the van der Waals case are $\lambda / kT_{cl} = 0.5$, $\alpha / \rho_{cl}T_{cl} = -0.05$, $\beta / k = -2$.

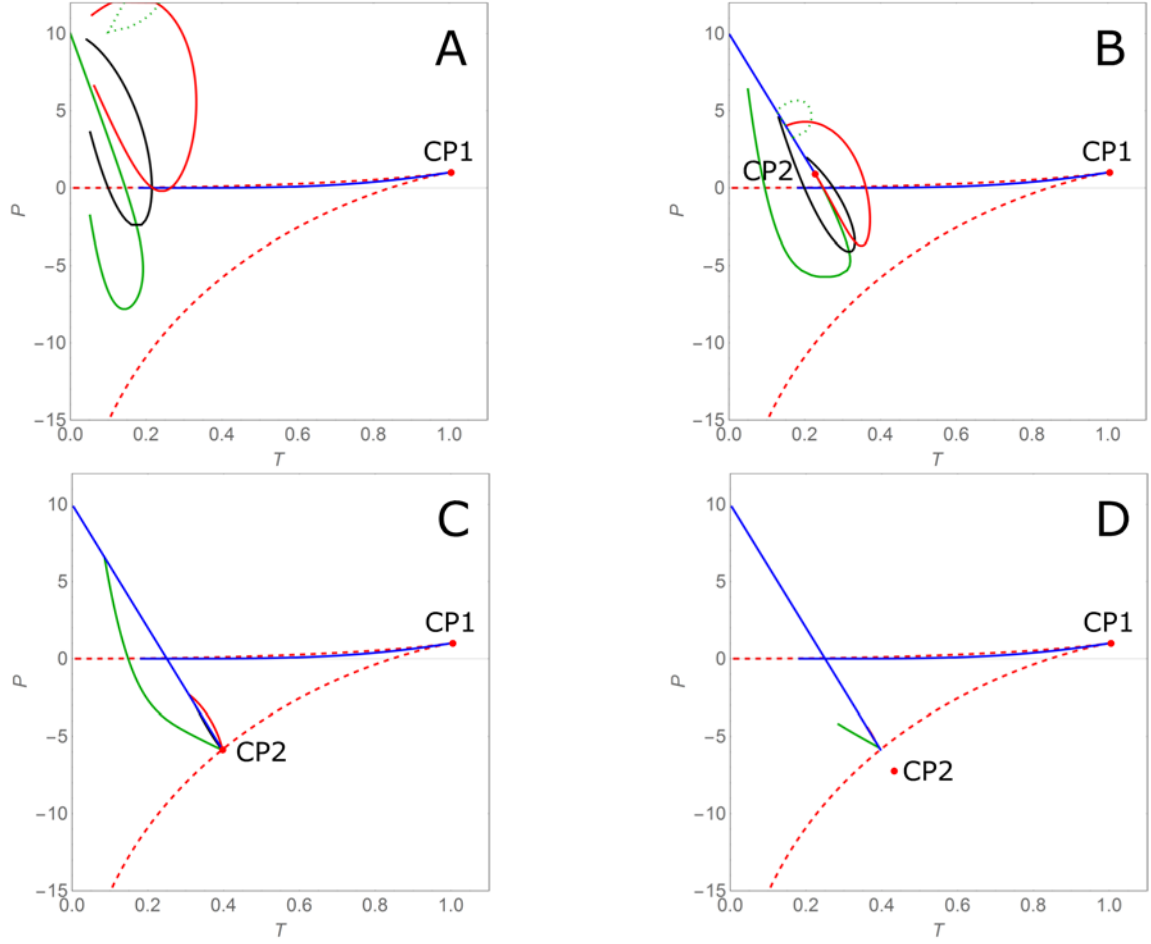


Figure S9. Evolution of the pattern of the extrema loci upon tuning the location of the liquid-liquid critical point, when state A is described with the van der Waals equation of state. Blue are liquid-vapor and liquid-liquid equilibrium lines, black is the density maximum or minimum; red is the isothermal compressibility maximum or minimum along isobars, green is the isobaric heat capacity maximum or minimum along isotherms; dashed green shows additional (shallow) extrema of the heat capacity unrelated to the liquid-liquid transition; dashed red are two branched of the liquid-vapor spinodal; red dot is the liquid-liquid critical point. (A) a singularity-free scenario – the critical point is at zero temperature; (B) a “regular” scenario – the critical point is at a positive pressure; (C) the critical point coincides with the absolute stability limit of the liquid state; (D) a critical point-free scenario – the “virtual” critical point is located in the unstable region.

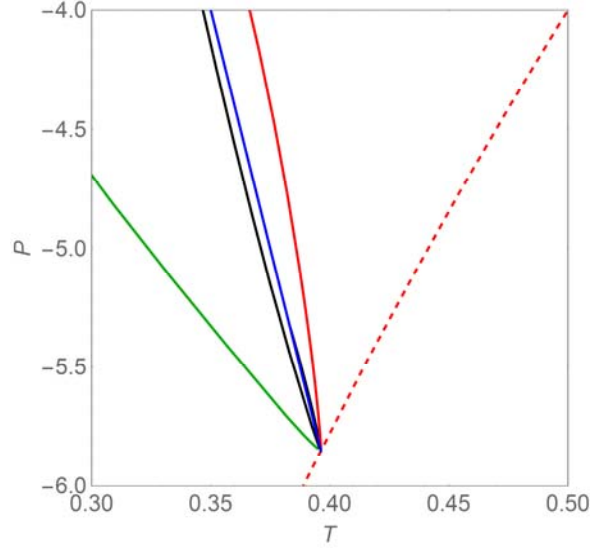


Fig. S10. Zooming the area near the liquid-liquid critical point shown in Figure S9C, which demonstrates the disappearance of the maximum density locus in the case where the critical coincides with the vapor-liquid spinodal point. The minimum density locus (to the left of the liquid-liquid coexistence) still exists.

5. Fluid polyamorphism: a singularity of the liquid-liquid coexistence (“bird’s beak”), the two-state model with van der Waals equation as the choice for state A

Gradual development of a singularity of the liquid-liquid coexistence when the metastable (with respect to vapor) liquid-liquid critical point approaches the absolute stability limit of liquid, is demonstrated in Fig. S11. Completely developed singularity (“bird’s beak”) is observed when the liquid-liquid critical point coincides with the liquid-vapor spinodal as shown in Fig. S11C and D. The character of the singularity for this (van der Waals) choice of state A is essentially similar to that observed for the lattice-gas choice of state A, confirming that the phenomenon is generic (compare with Fig. 5b of the main manuscript).

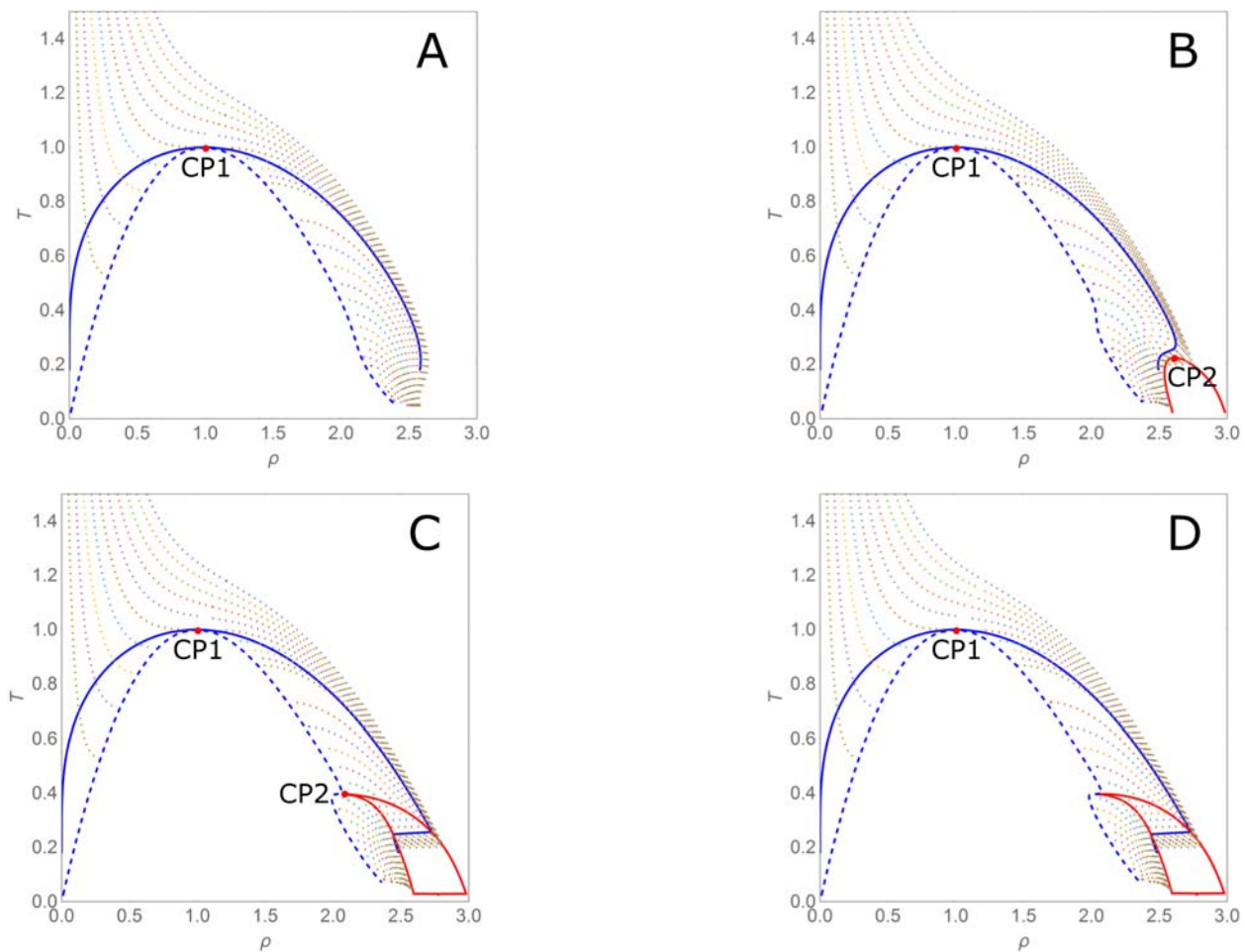


Figure S11. A singularity (“bird’s beak”) in the liquid-liquid coexistence curve develops when the critical point approaches with the liquid-vapor spinodal (the van der Waals choice for state A). The four $T - \rho$ diagrams correspond to the four cases shown in Fig. S9. Blue curve is the vapor-liquid coexistence; red is the liquid-liquid coexistence; dashed blue is the liquid-vapor spinodal; multicolor curves are selected isobars.

6. Fluid polyamorphism: phase separation near the tricritical point of a polymerization transition

The phase separation of a polymer solution into the pure monomer solvent and concentrated polymer solution in the limit of the infinite degree of polymerization is obtained from the condition

$$-kT \ln(1-x) - kTx - \frac{1}{2} \Theta x^2 = 0. \quad (\text{S19})$$

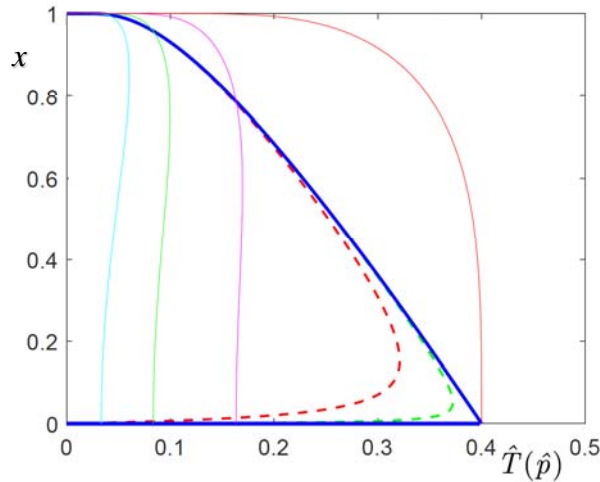


Fig. S12. Two solutions of Eq. (19) for the fraction of polymerized molecules (x) below the tricritical (theta) point in the limit of infinite degree of polymerization. Blue is the liquid-liquid coexistence. Dashed curves correspond to finite degree of polymerization (red $N = 10$, green $N = 30$). Multicolor curves are selected isobars.

References

1. J. Frenkel, *Kinetic Theory of Liquids* (Clarendon Press, Oxford, 1946).
2. C. N. Yang and T. D. Lee, Phys. Rev. **87**, 404 and 410 (1952).
3. K. Huang, *Statistical Mechanics*, 2nd edn. (John Wiley & Sons, Inc., New York, 1987).
4. E. Ising, Z. Phys. **31**, 253 (1925).
5. S. G. Brush, Rev. Mod. Phys. **39**, 883 (1967)
6. S. Moghaddam, Y. C. Kim, and M. E. Fisher, J. Phys. Chem. B **109**, 6824 (2005).